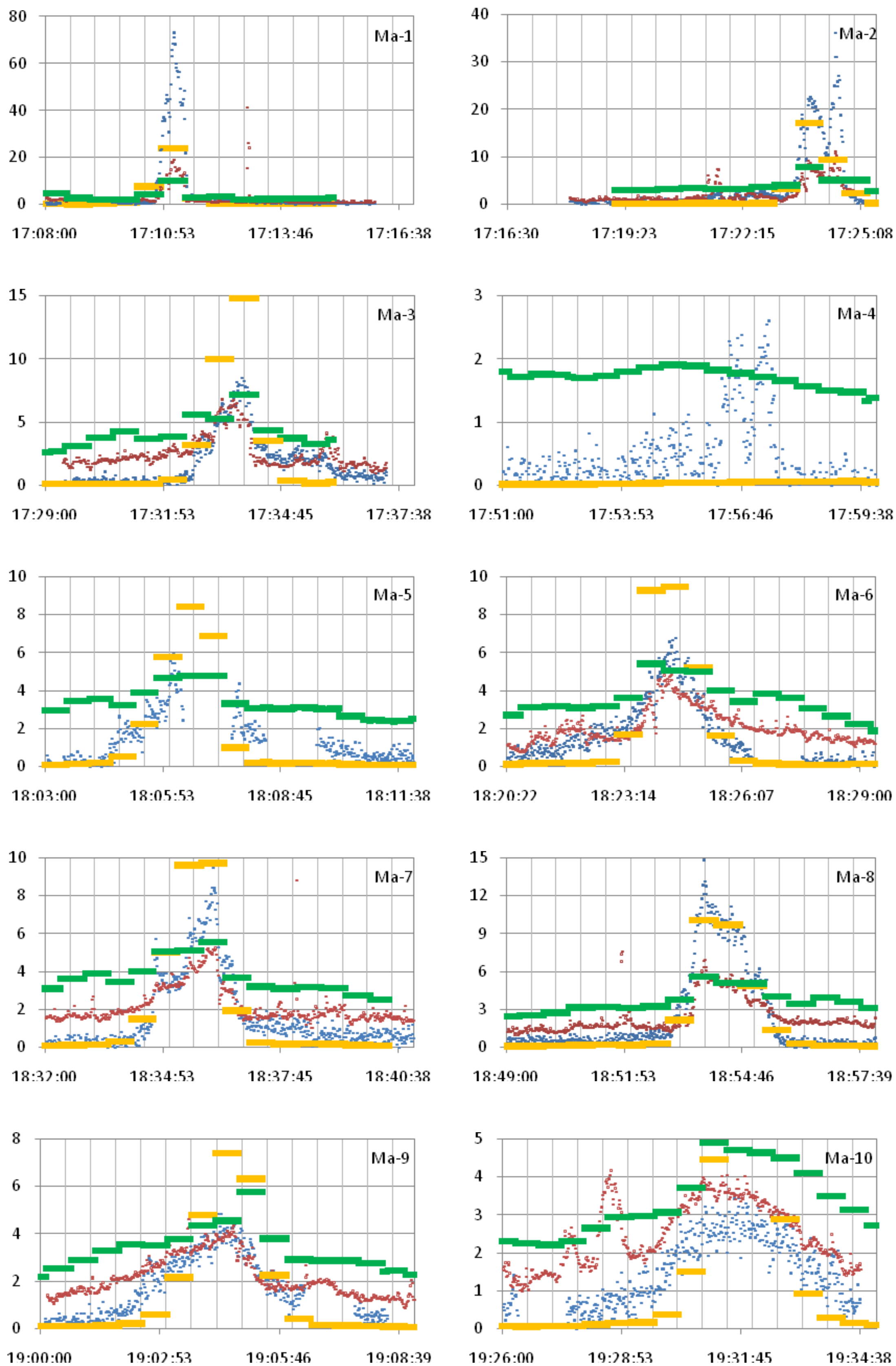
Ma-1
80
60
40
20
0
17:08:00
17:10:53
17:13:46
17:16:38
Ma-2
40
30
20
10
0
17:16:30
17:19:23
17:22:15
17:25:08
Ma-3
15
10
5
0
17:29:00
17:31:53
17:34:45
17:37:38
Ma-4
3
2
1
0
17:51:00
17:53:53
17:56:46
17:59:38
Ma-5
10
8
6
4
2
0
18:03:00
18:05:53
18:08:45
18:11:38
Ma-6
10
8
6
4
2
0
18:20:22
18:23:14
18:26:07
18:29:00
Ma-7
10
8
6
4
2
0
18:32:00
18:34:53
18:37:45
18:40:38
Ma-8
15
12
9
6
3
0
18:49:00
18:51:53
18:54:46
18:57:39
Ma-9
8
6
4
2
0
19:00:00
19:02:53
19:05:46
19:08:39
Ma-10
5
4
3
2
1
0
19:26:00
19:28:53
19:31:45
19:34:38

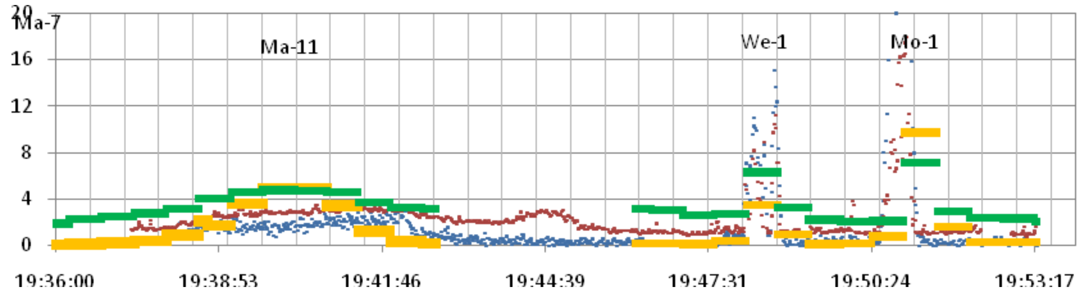
20
Ma-7
16
12
8
4
0
Ma-11
We-1
Mo-1
19:36:00
19:38:53
19:41:46
19:44:39
19:47:31
19:50:24
19:53:17

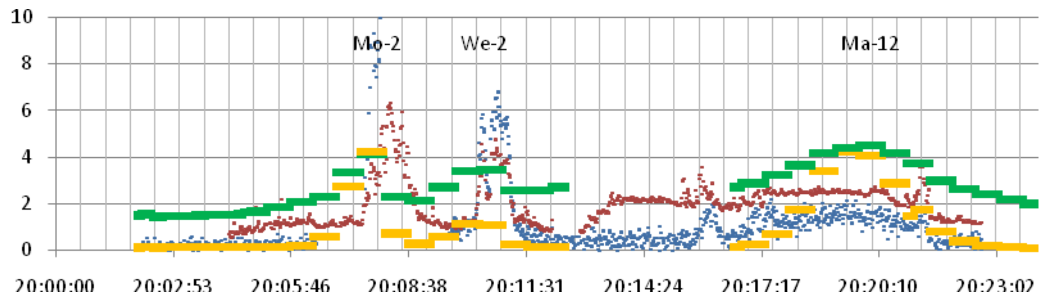
10
8
6
4
2
0
Mo-2
We-2
Ma-12
20:00:00
20:02:53
20:05:46
20:08:38
20:11:31
20:14:24
20:17:17
20:20:10
20:23:02

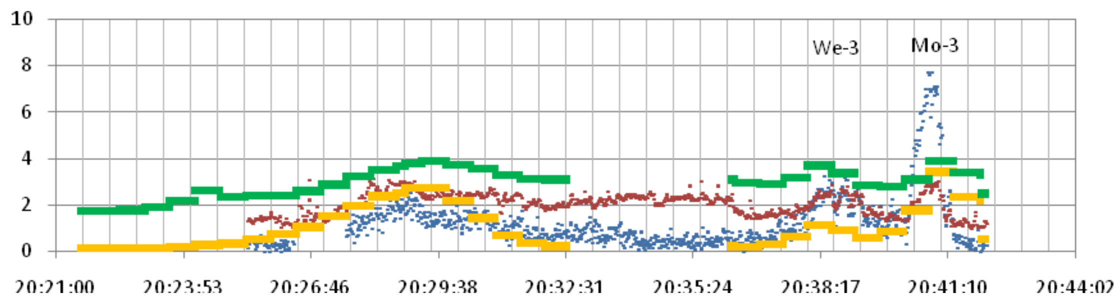
10
8
6
4
2
0
We-3
Mo-3
20:21:00
20:23:53
20:26:46
20:29:38
20:32:31
20:35:24
20:38:17
20:41:10
20:44:02

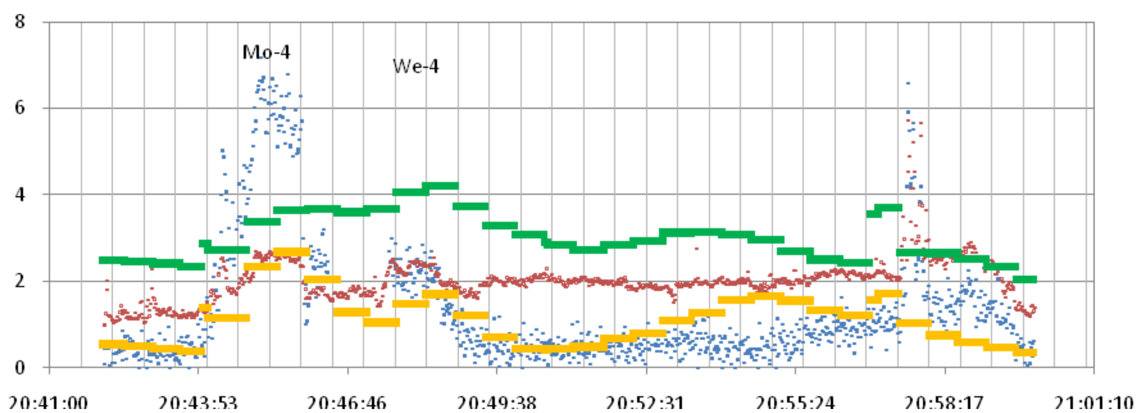
8
6
4
2
0
Mo-4
We-4
20:41:00
20:43:53
20:46:46
20:49:38
20:52:31
20:55:24
20:58:17
21:01:10

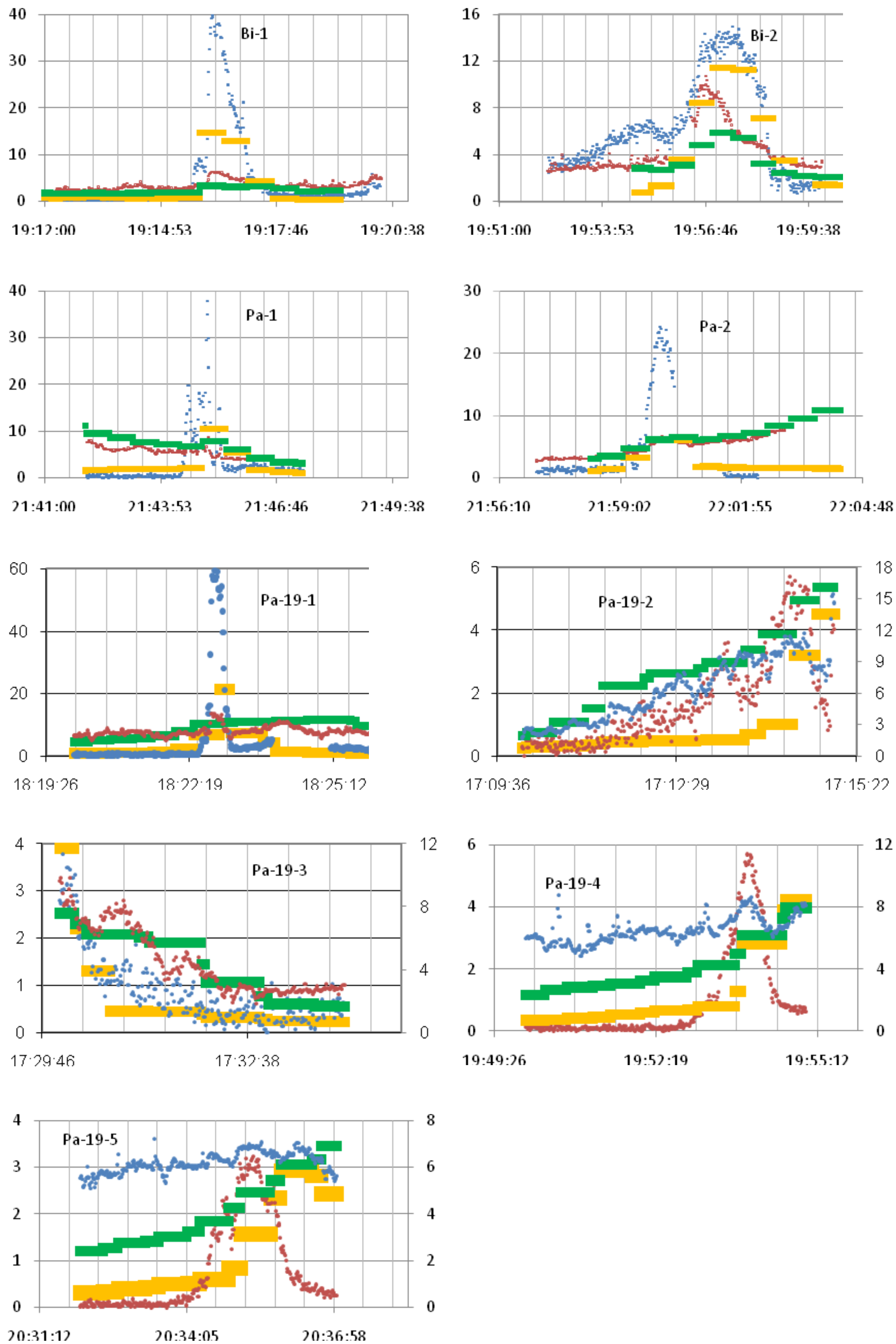
Bi-1
19:12:00
19:14:53
19:17:46
19:20:38
Bi-2
19:51:00
19:53:53
19:56:46
19:59:38
Pa-1
21:41:00
21:43:53
21:46:46
21:49:38
Pa-2
21:56:10
21:59:02
22:01:55
22:04:48
Pa-19-1
18:19:26
18:22:19
18:25:12
Pa-19-2
17:09:36
17:12:29
17:15:22
Pa-19-3
17:29:46
17:32:38
Pa-19-4
19:49:26
19:52:19
19:55:12
Pa-19-5
20:31:12
20:34:05
20:36:58

Fig. S1. Comparison of modeled $SO_2$ (yellow flat line) and $NO_y$ (green flat line) to the observed $SO_2$ (blue dot) and $NO_y$ (red dots) at each plume transect on September 16, 19 and 25. Horizontal coordinate is time scale in GMT (local time = GMT - 6 hours) and vertical coordinate is concentration (ppb). Transect names listed in Table S3 of the manuscript are labled in each subplot.

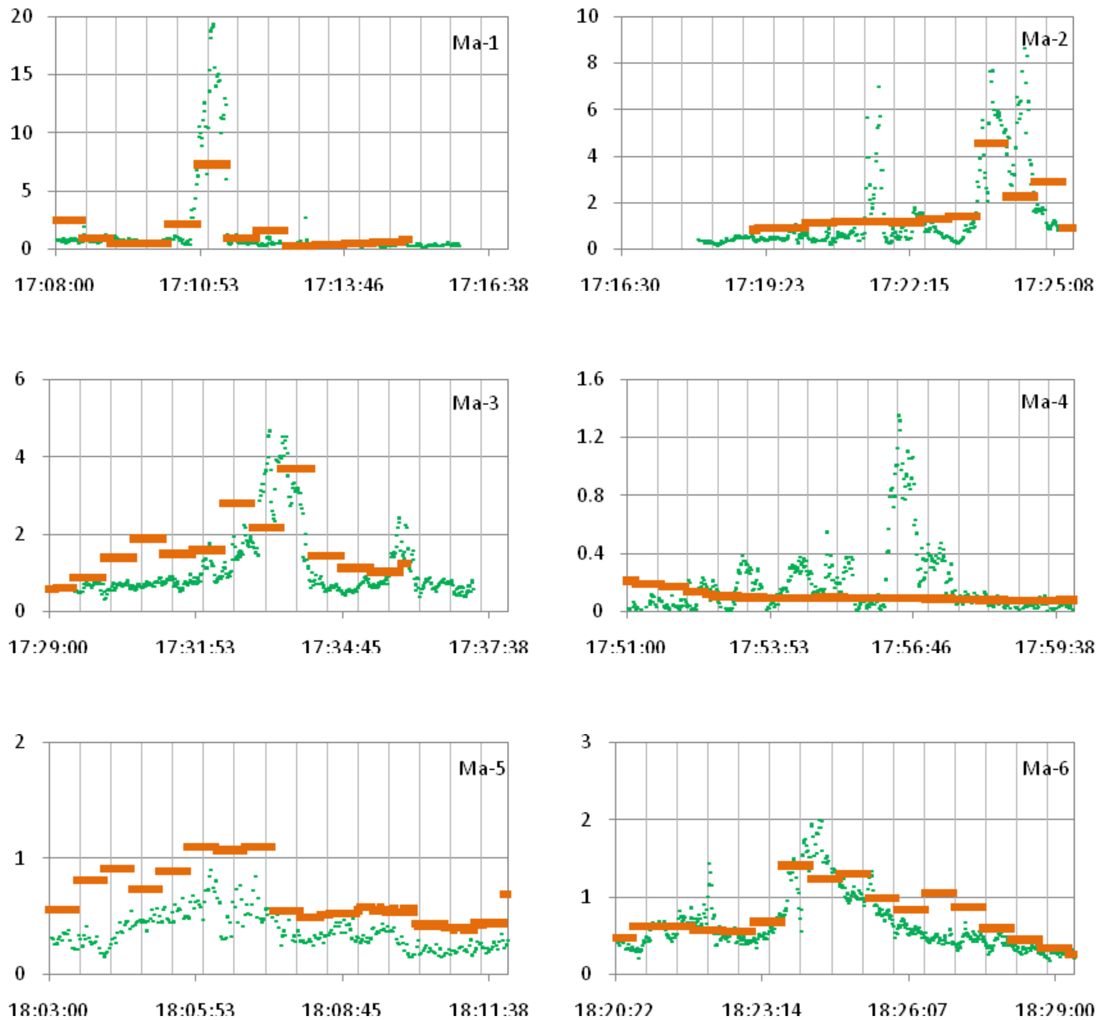

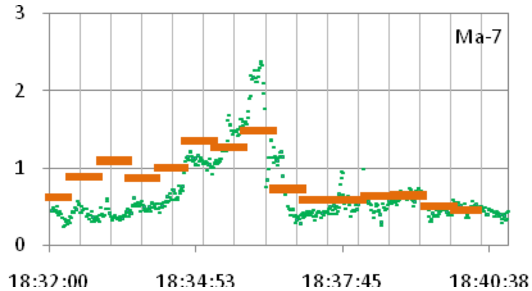
Ma-7
3
2
1
0
18:32:00
18:34:53
18:37:45
18:40:38

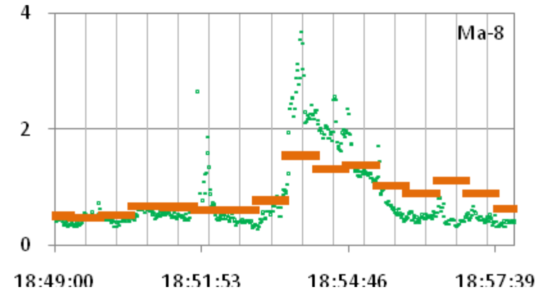
Ma-8
4
2
0
18:49:00
18:51:53
18:54:46
18:57:39

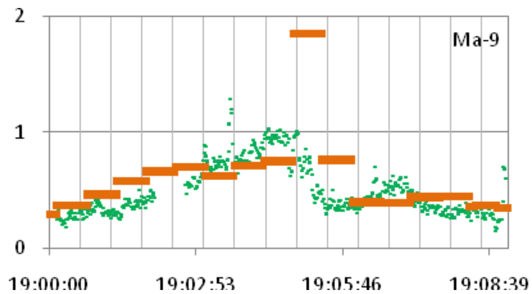
Ma-9
2
1
0
19:00:00
19:02:53
19:05:46
19:08:39

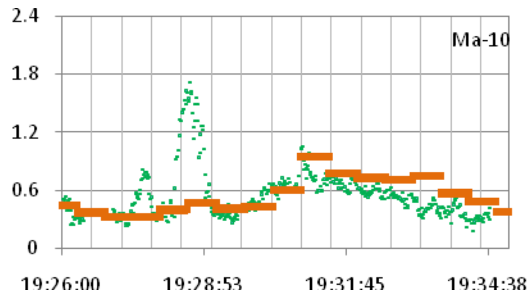
Ma-10
2.4
1.8
1.2
0.6
0
19:26:00
19:28:53
19:31:45
19:34:38

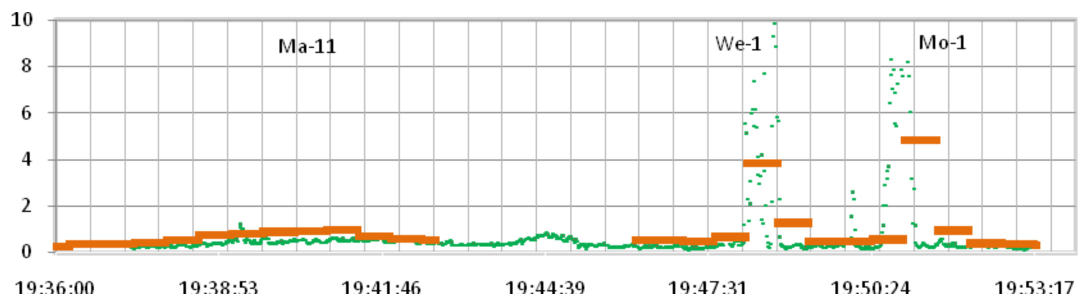
Ma-11
We-1
Mo-1
10
8
6
4
2
0
19:36:00
19:38:53
19:41:46
19:44:39
19:47:31
19:50:24
19:53:17

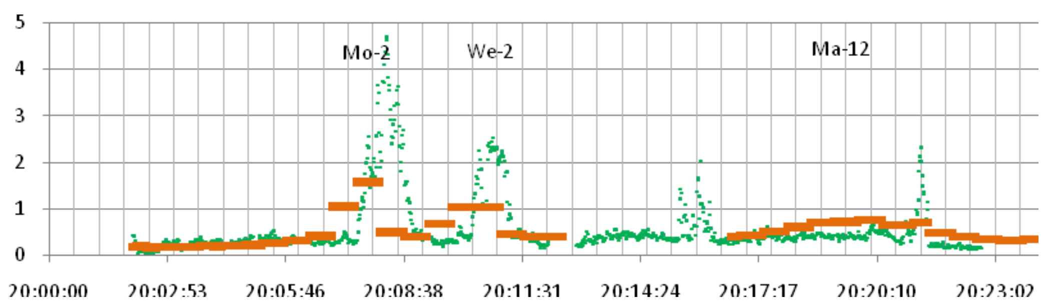
Mo-2
We-2
Ma-12
5
4
3
2
1
0
20:00:00
20:02:53
20:05:46
20:08:38
20:11:31
20:14:24
20:17:17
20:20:10
20:23:02

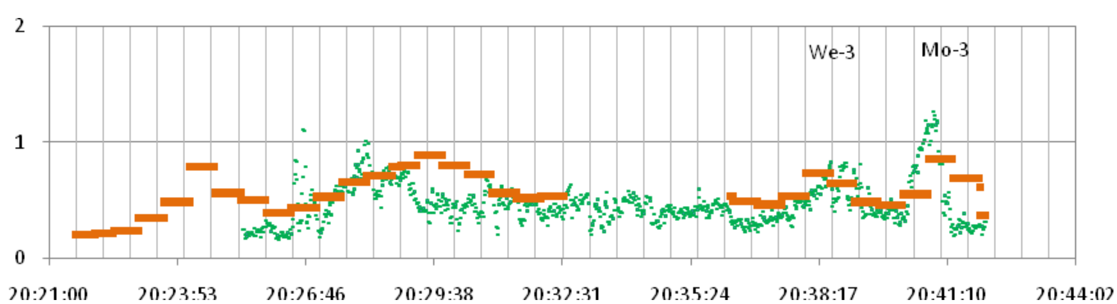
We-3
Mo-3
2
1
0
20:21:00
20:23:53
20:26:46
20:29:38
20:32:31
20:35:24
20:38:17
20:41:10
20:44:02

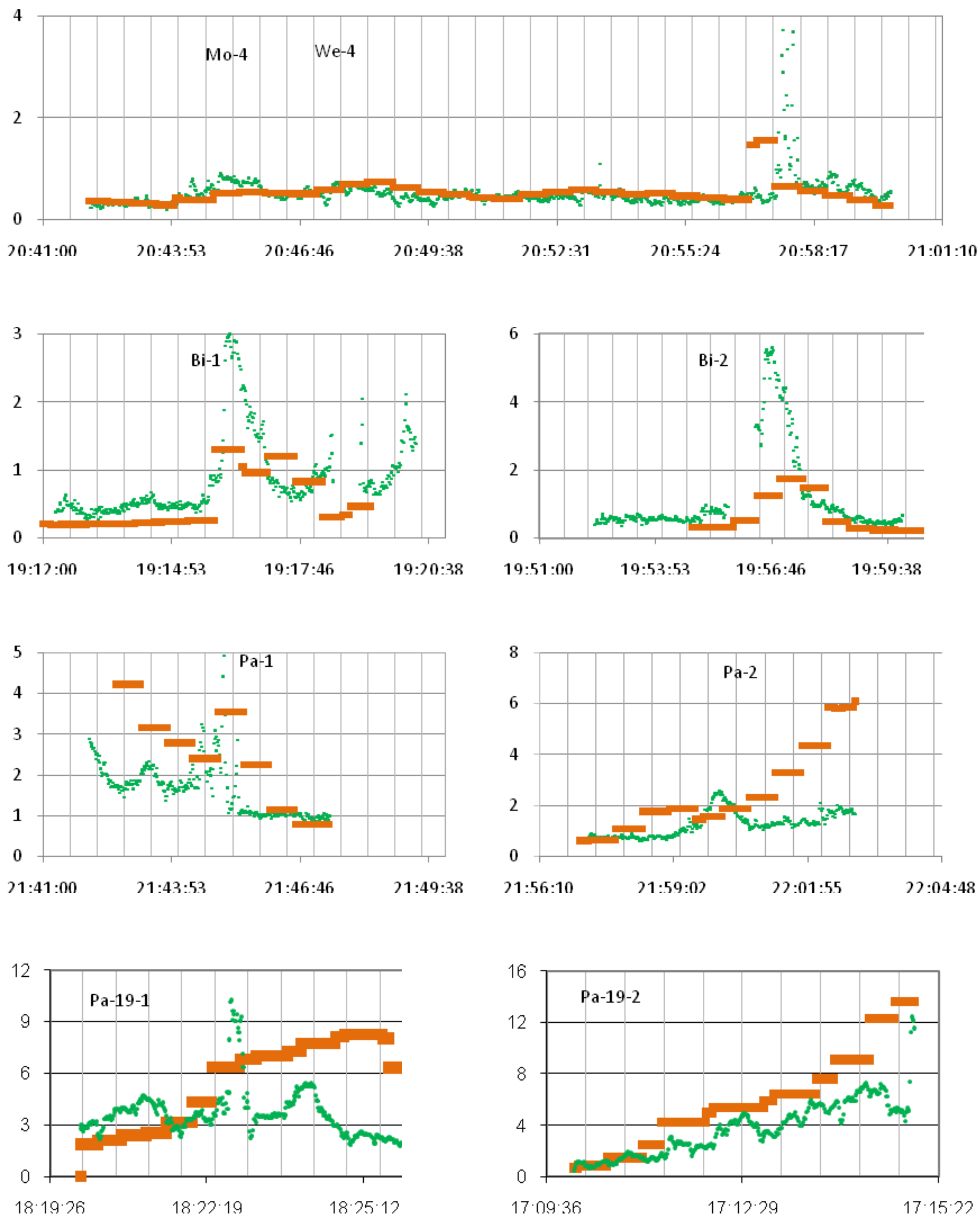
Mo-4
We-4
0
2
4
20:41:00
20:43:53
20:46:46
20:49:38
20:52:31
20:55:24
20:58:17
21:01:10
Bi-1
0
1
2
3
19:12:00
19:14:53
19:17:46
19:20:38
Bi-2
0
2
4
6
19:51:00
19:53:53
19:56:46
19:59:38
Pa-1
0
1
2
3
4
5
21:41:00
21:43:53
21:46:46
21:49:38
Pa-2
0
2
4
6
8
21:56:10
21:59:02
22:01:55
22:04:48
Pa-19-1
0
3
6
9
12
18:19:26
18:22:19
18:25:12
Pa-19-2
0
4
8
12
16
17:09:36
17:12:29
17:15:22

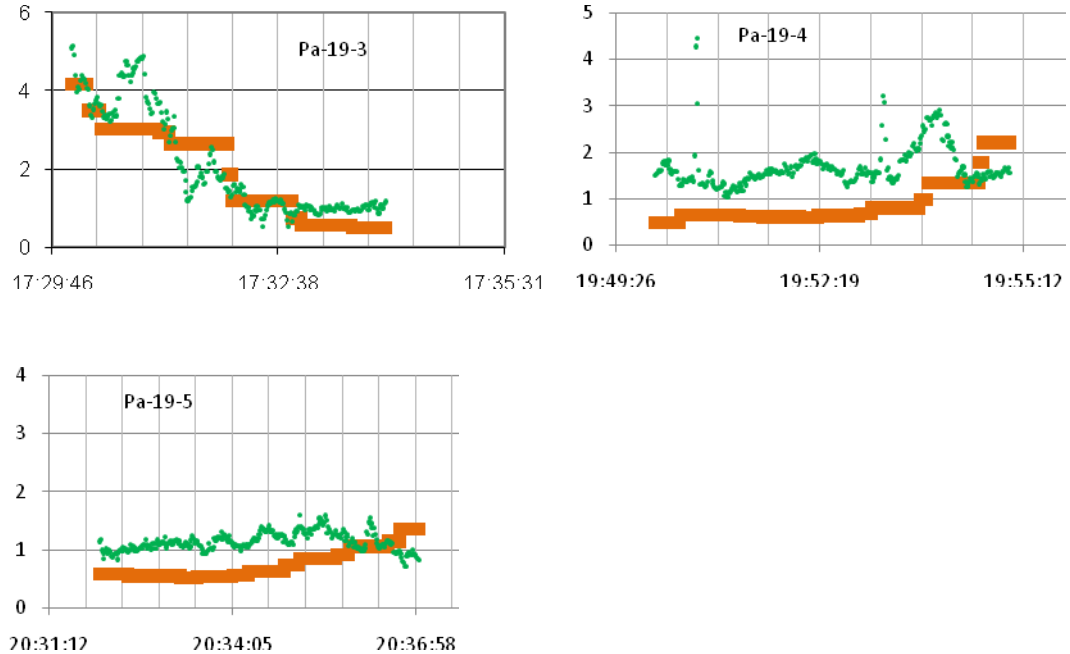


Fig. S2. Comparison of the modeled $NO_x$ (orange flat line) to the observed $NO_x$ (green dot) at each plume transect on September 16, 19 and 25. Horizontal coordinate is time in GMT (local time = GMT - 6 hours) and vertical coordinate is concentration (ppb). Transect names listed in Table S3 of the manuscript are labled in each subplot.

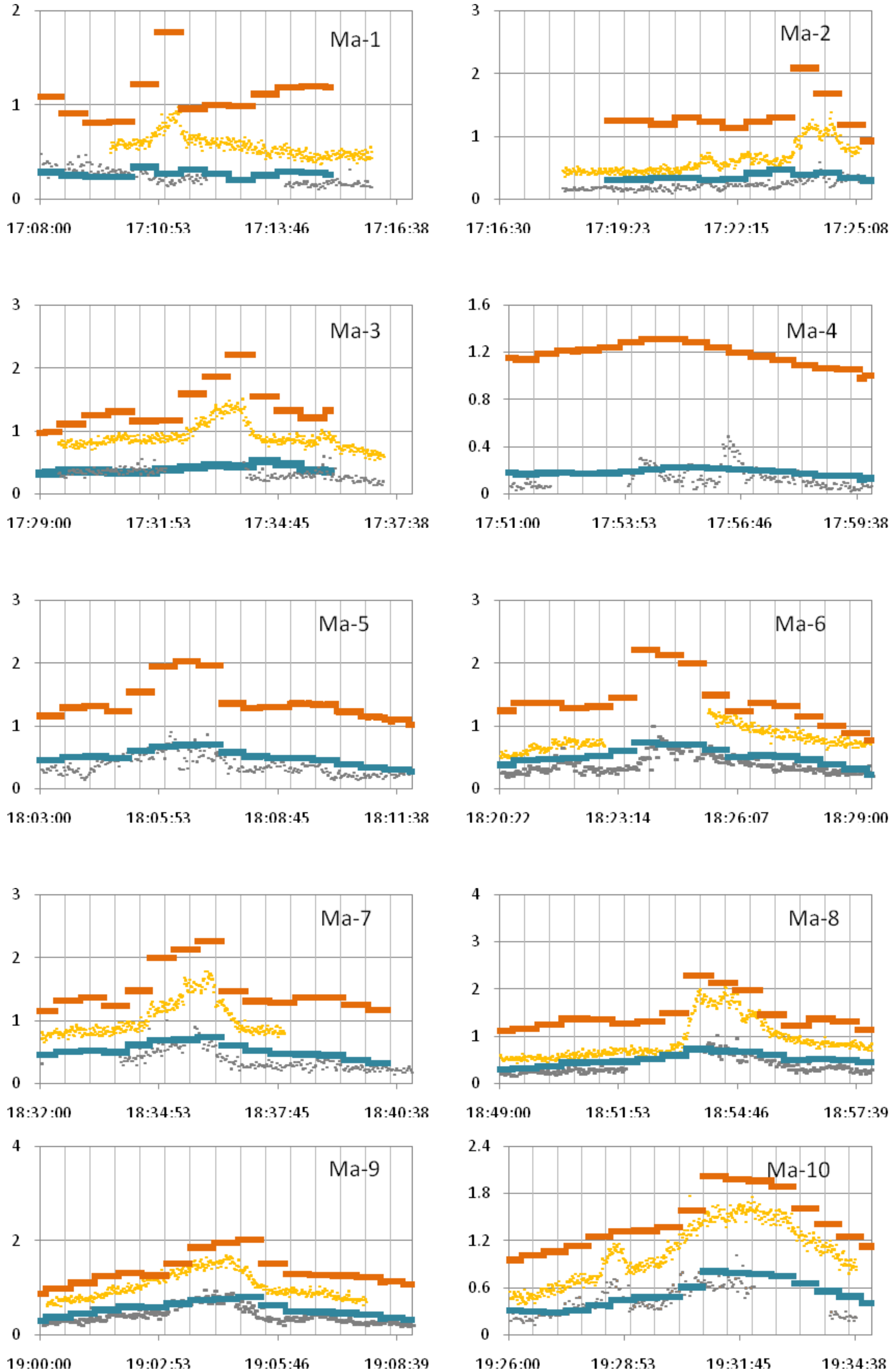
Ma-1
2
1
0
17:08:00
17:10:53
17:13:46
17:16:38
Ma-2
3
2
1
0
17:16:30
17:19:23
17:22:15
17:25:08
Ma-3
3
2
1
0
17:29:00
17:31:53
17:34:45
17:37:38
Ma-4
1.6
1.2
0.8
0.4
0
17:51:00
17:53:53
17:56:46
17:59:38
Ma-5
3
2
1
0
18:03:00
18:05:53
18:08:45
18:11:38
Ma-6
3
2
1
0
18:20:22
18:23:14
18:26:07
18:29:00
Ma-7
3
2
1
0
18:32:00
18:34:53
18:37:45
18:40:38
Ma-8
4
3
2
1
0
18:49:00
18:51:53
18:54:46
18:57:39
Ma-9
4
2
0
19:00:00
19:02:53
19:05:46
19:08:39
Ma-10
2.4
1.8
1.2
0.6
0
19:26:00
19:28:53
19:31:45
19:34:38

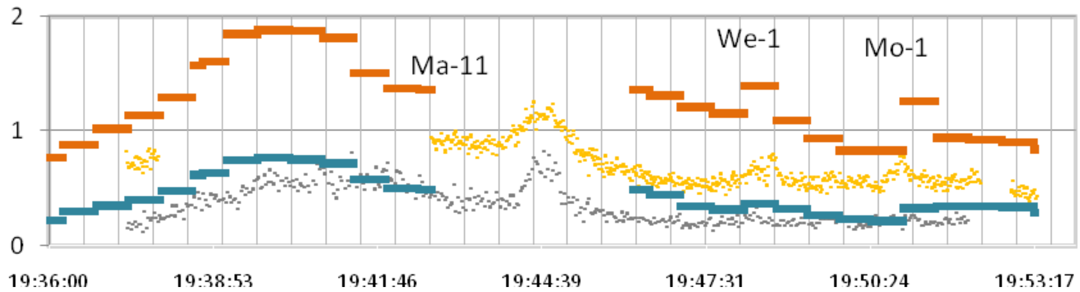
Ma-11
We-1
Mo-1
0
1
2
19:36:00
19:38:53
19:41:46
19:44:39
19:47:31
19:50:24
19:53:17

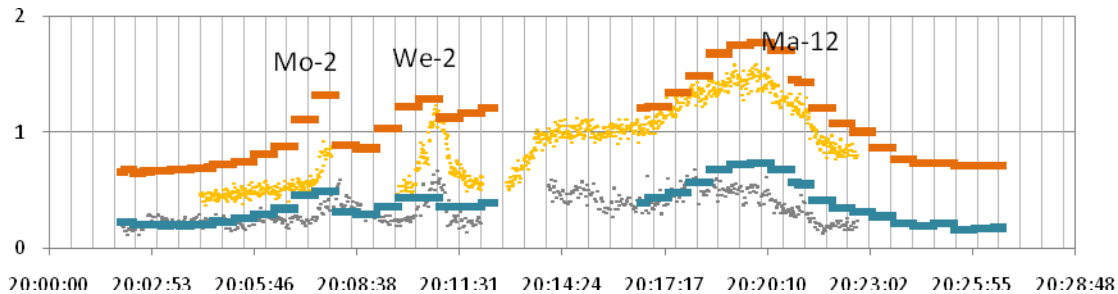
Mo-2
We-2
Ma-12
0
1
2
20:00:00
20:02:53
20:05:46
20:08:38
20:11:31
20:14:24
20:17:17
20:20:10
20:23:02
20:25:55
20:28:48

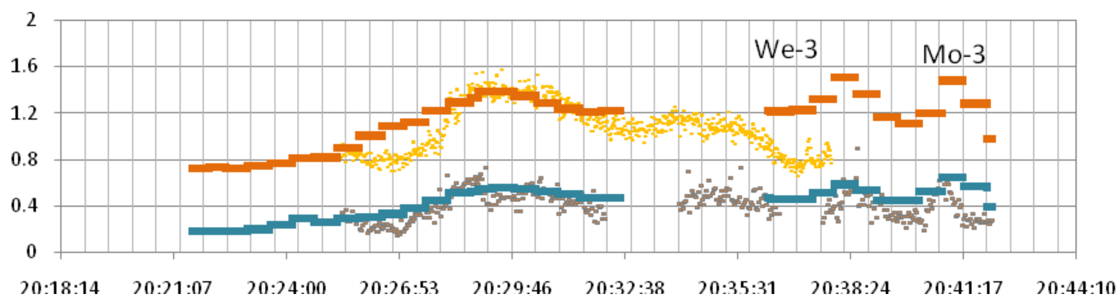
We-3
Mo-3
0
0.4
0.8
1.2
1.6
2
20:18:14
20:21:07
20:24:00
20:26:53
20:29:46
20:32:38
20:35:31
20:38:24
20:41:17
20:44:10

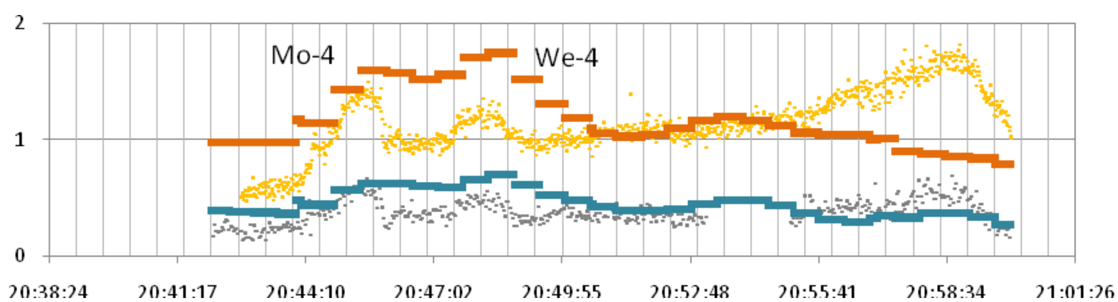
Mo-4
We-4
0
1
2
20:38:24
20:41:17
20:44:10
20:47:02
20:49:55
20:52:48
20:55:41
20:58:34
21:01:26

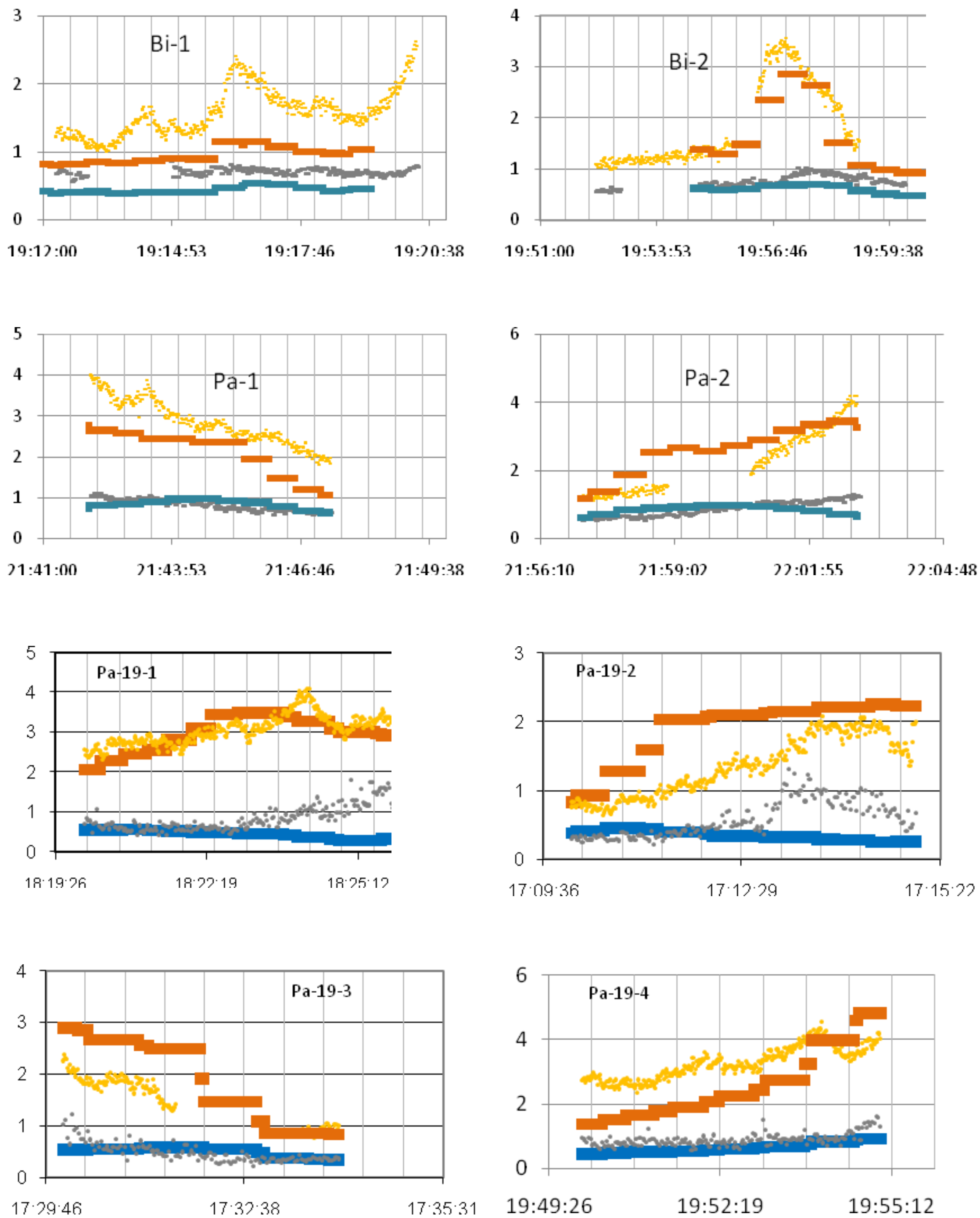
Bi-1
0
1
2
3
19:12:00
19:14:53
19:17:46
19:20:38
Bi-2
0
1
2
3
4
19:51:00
19:53:53
19:56:46
19:59:38
Pa-1
0
1
2
3
4
5
21:41:00
21:43:53
21:46:46
21:49:38
Pa-2
0
2
4
6
21:56:10
21:59:02
22:01:55
22:04:48
Pa-19-1
0
1
2
3
4
5
18:19:26
18:22:19
18:25:12
Pa-19-2
0
1
2
3
17:09:36
17:12:29
17:15:22
Pa-19-3
0
1
2
3
4
17:29:46
17:32:38
17:35:31
Pa-19-4
0
2
4
6
19:49:26
19:52:19
19:55:12

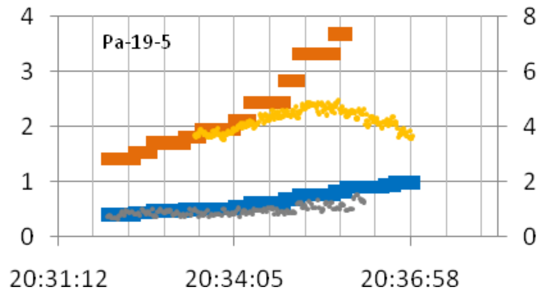


Fig. S3. Comparison of the modeled $HNO_3$ (orange flat line) and PAN (aqua flat line) to the observed $HNO_3$ (yellow dot) and PAN (gray dot) at each plume transect on September 16, 19 and 25. Horizontal coordinate is time in GMT (local time = GMT - 6 hours) and vertical coordinate is concentration (ppb). Transect names listed in Table S3 of the manuscript are labeled in each subplot.

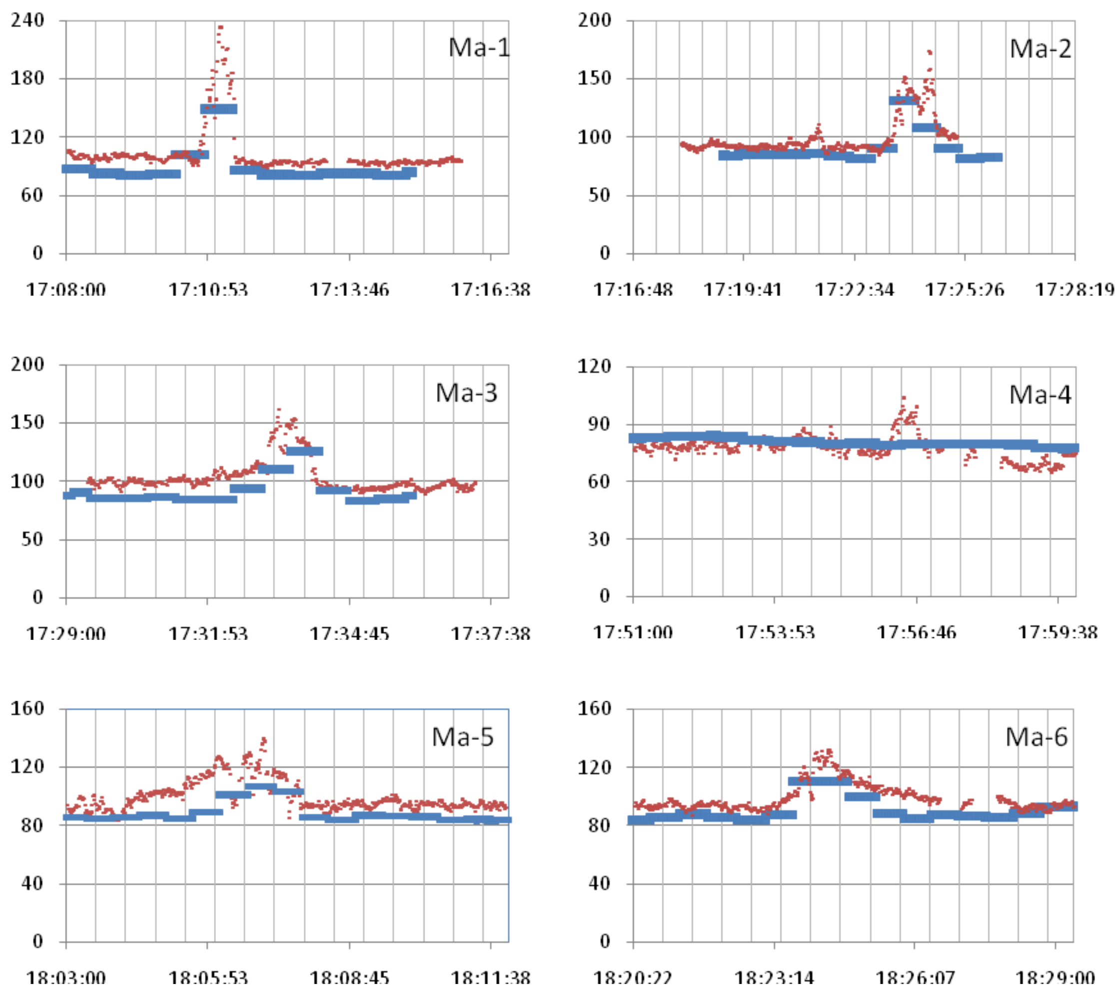

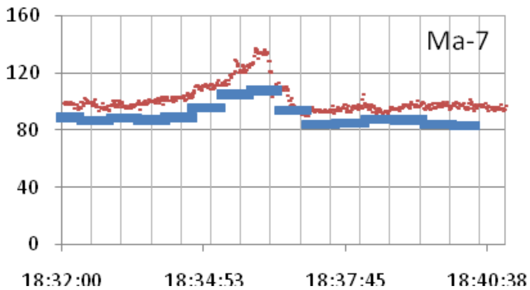
Ma-7
160
120
80
40
0
18:32:00
18:34:53
18:37:45
18:40:38

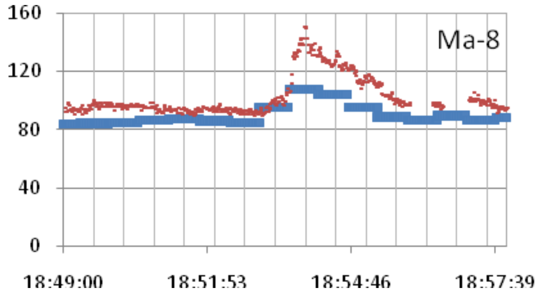
Ma-8
160
120
80
40
0
18:49:00
18:51:53
18:54:46
18:57:39

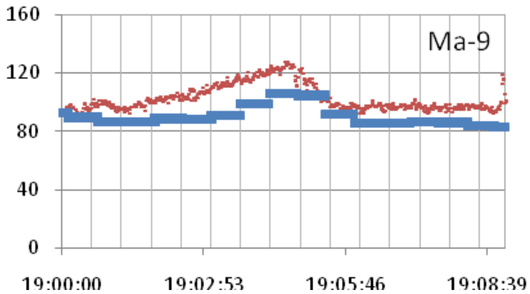
Ma-9
160
120
80
40
0
19:00:00
19:02:53
19:05:46
19:08:39

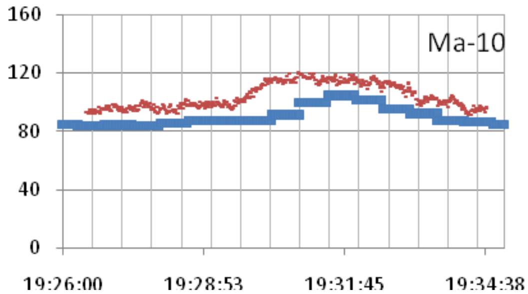
Ma-10
160
120
80
40
0
19:26:00
19:28:53
19:31:45
19:34:38

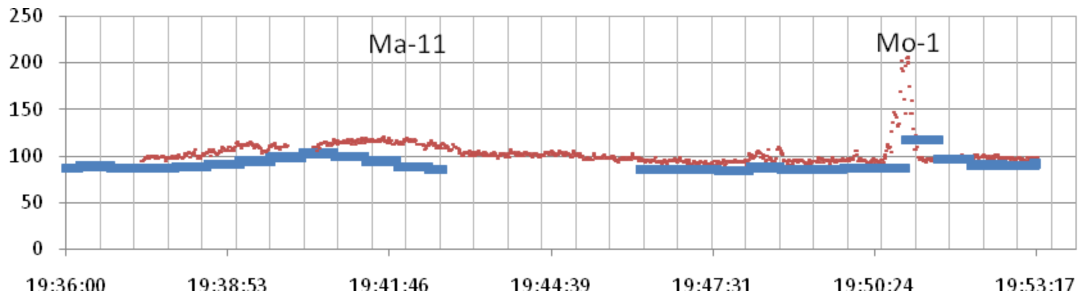
Ma-11
Mo-1
250
200
150
100
50
0
19:36:00
19:38:53
19:41:46
19:44:39
19:47:31
19:50:24
19:53:17

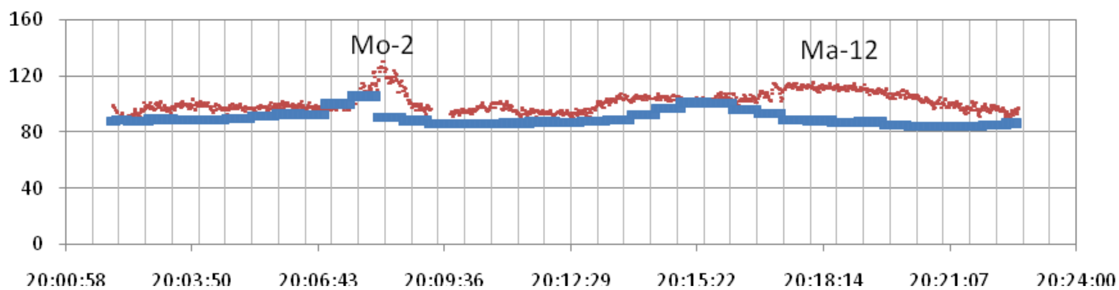
Mo-2
Ma-12
160
120
80
40
0
20:00:58
20:03:50
20:06:43
20:09:36
20:12:29
20:15:22
20:18:14
20:21:07
20:24:00

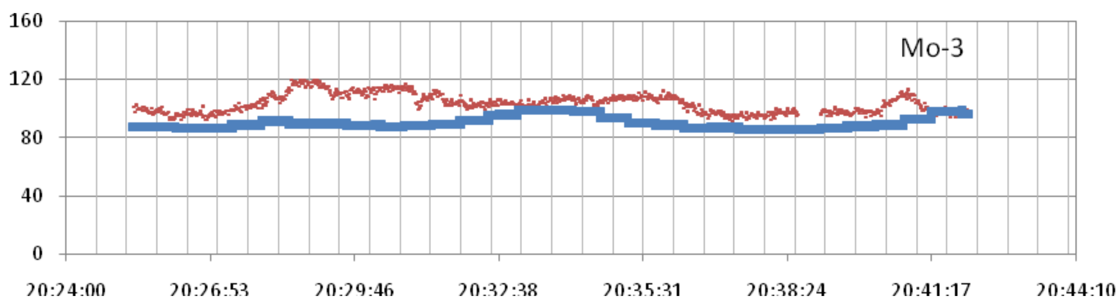
Mo-3
160
120
80
40
0
20:24:00
20:26:53
20:29:46
20:32:38
20:35:31
20:38:24
20:41:17
20:44:10

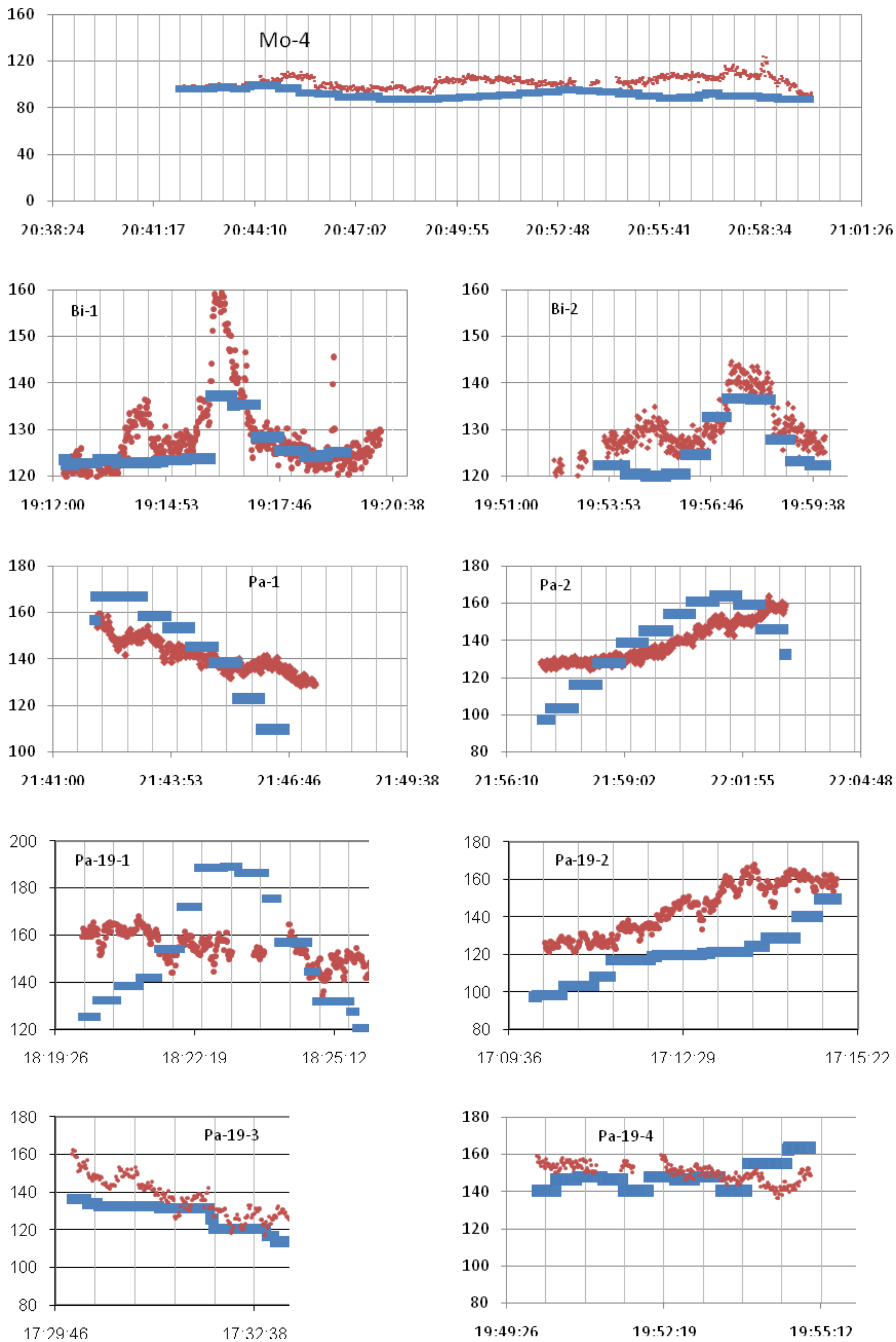
Mo-4
160
120
80
40
0
20:38:24
20:41:17
20:44:10
20:47:02
20:49:55
20:52:48
20:55:41
20:58:34
21:01:26
Bi-1
160
150
140
130
120
19:12:00
19:14:53
19:17:46
19:20:38
Bi-2
160
150
140
130
120
19:51:00
19:53:53
19:56:46
19:59:38
Pa-1
180
160
140
120
100
21:41:00
21:43:53
21:46:46
21:49:38
Pa-2
180
160
140
120
100
80
21:56:10
21:59:02
22:01:55
22:04:48
Pa-19-1
200
180
160
140
120
18:19:26
18:22:19
18:25:12
Pa-19-2
180
160
140
120
100
80
17:09:36
17:12:29
17:15:22
Pa-19-3
180
160
140
120
100
80
17:29:46
17:32:38
Pa-19-4
180
160
140
120
100
80
19:49:26
19:52:19
19:55:12

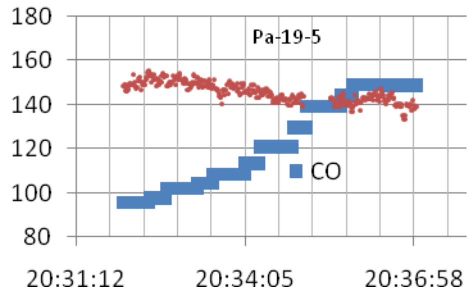


Fig. S4. Comparison of the modeled CO (blue flat line) to the observed CO (red dot) at each plume transect on September 16, 19 and 25. Horizontal coordinate is time in GMT (local time = GMT - 6 hours) and vertical coordinate is concentration (ppb). Transect names listed in Table S3 of the manuscript are labled in each subplot.

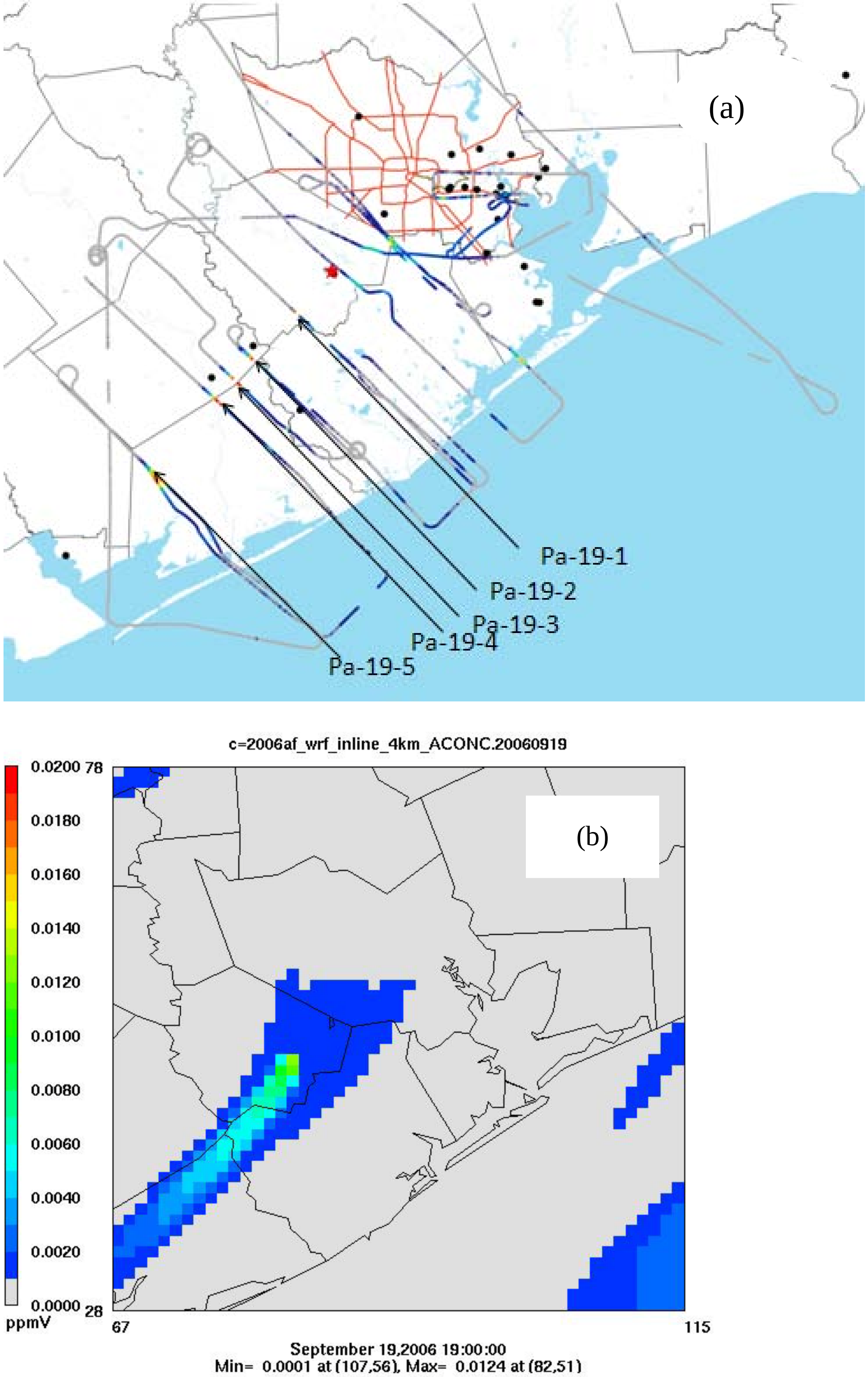


Fig. S5. (a) Observed PPPs of Parish on September 19, 2006. The red star show the locations of the Parish plant. (b) Simulated PPPs of Parish at 19:00 GMT (local time: 13:00)

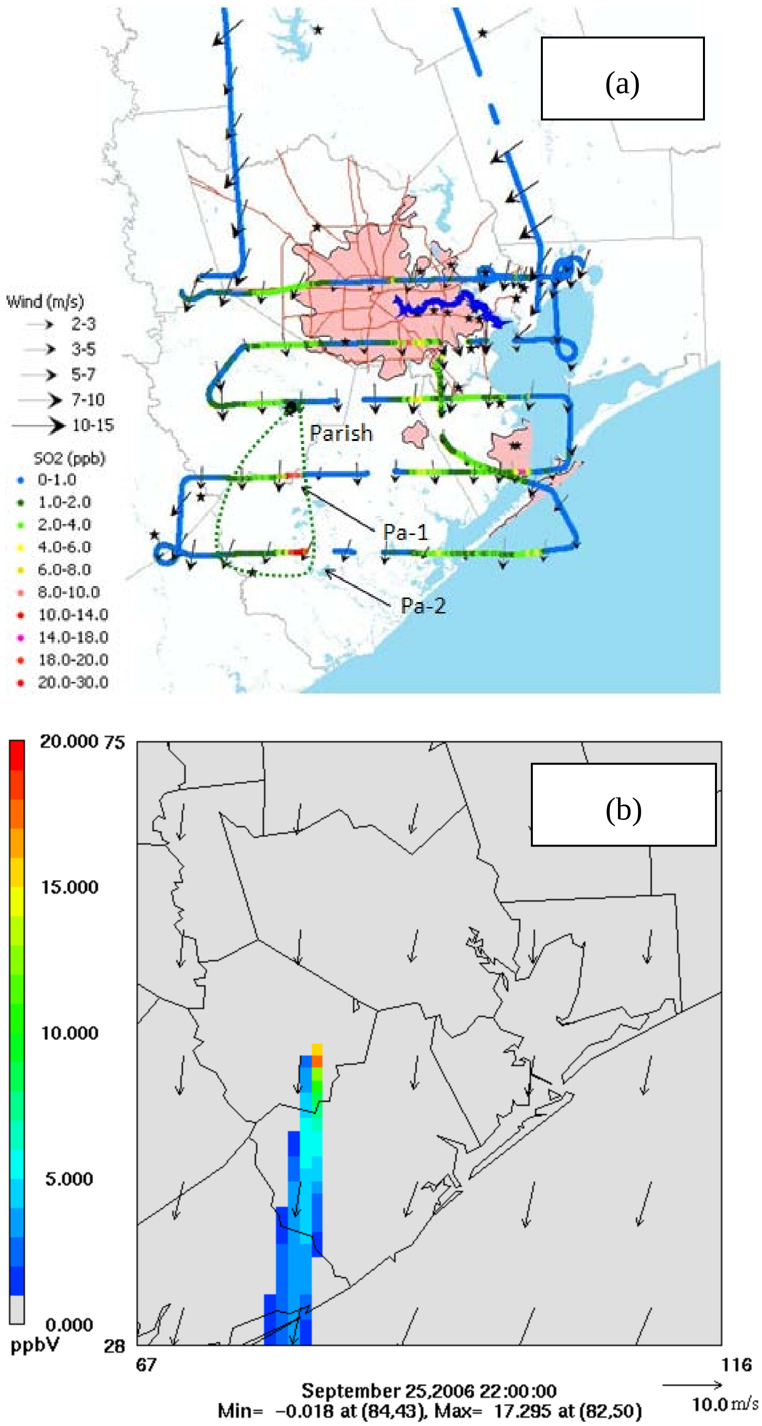
(a)
Wind (m/s)
2-3
3-5
5-7
7-10
10-15
SO2 (ppb)
0-1.0
1.0-2.0
2.0-4.0
4.0-6.0
6.0-8.0
8.0-10.0
10.0-14.0
14.0-18.0
18.0-20.0
20.0-30.0
Parish
Pa-1
Pa-2
(b)
20.000
15.000
10.000
5.000
0.000
ppbV
75
28
67
116
September 25,2006 22:00:00
Min= -0.018 at (84,43), Max= 17.295 at (82,50)
10.0 m/s

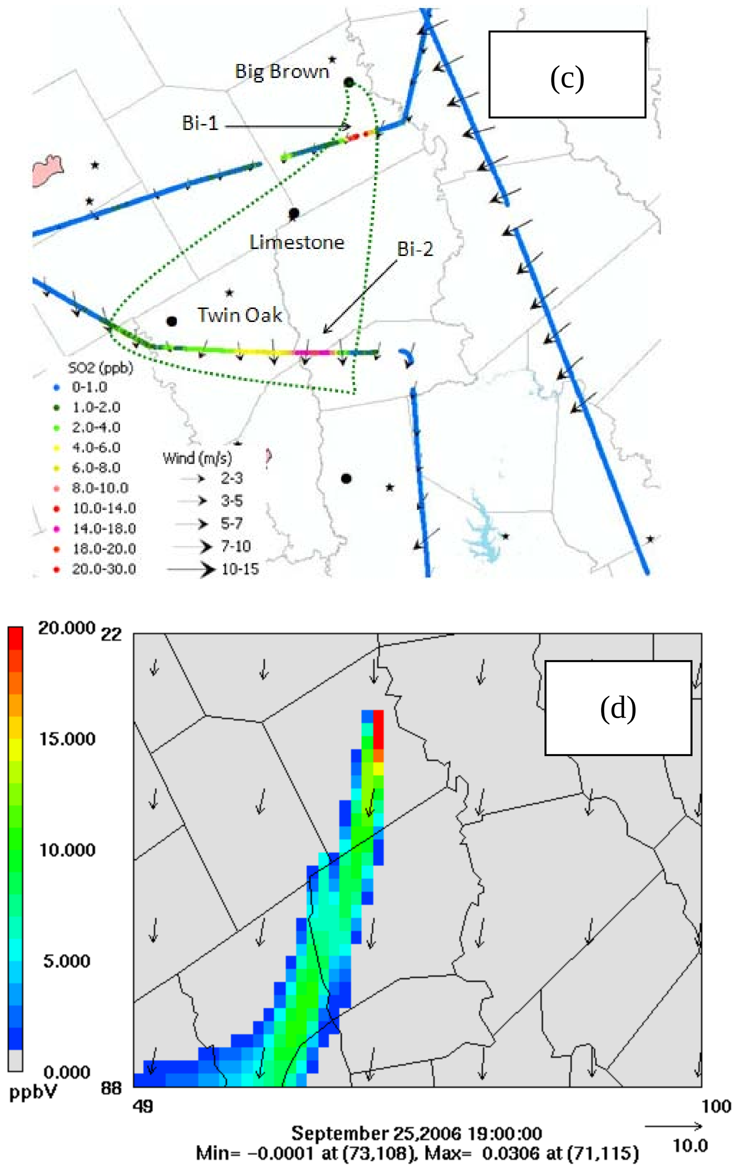


Fig. S6. (a) Observed PPPs of Parish on September 25, 2006. The black dots show the locations of the power plants. PPPs are identified by measured $SO_2$ enhancement (color gradient in the figure), are outlined using green dash lines. Measured wind vectors are presented on the plume transect. (b) Simulated PPPs of Parish at 22:00 GMT (local time: 16:00). (c) Observed PPPs of Big Brown and Limestone on September 25, 2006. The black dots show the locations of the power plants. PPPs are identified by measured $SO_2$ enhancement (color gradient in the figure), are outlined using green dash lines. Measured winds vectors are presented on the plume transect. (d) Simulated PPPs of Big Brown and Limestone at 19:00 GMT (local time: 13:00)

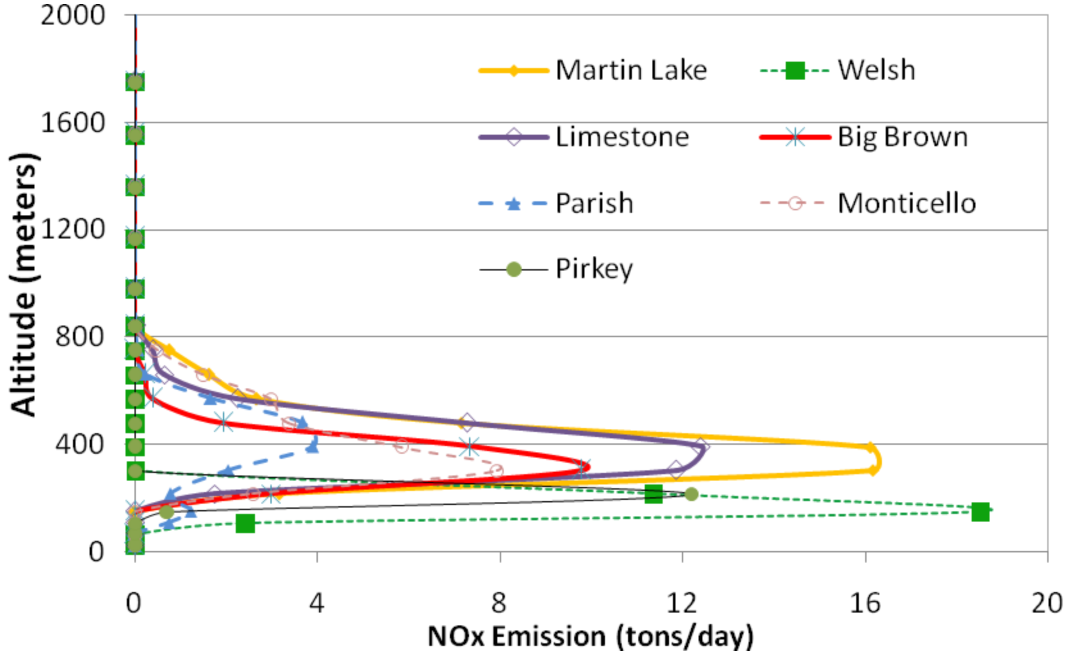


Fig. S7. Vertical distribution of $NO_x$ for power plants simulated by CMAQ inline v4.7 on the day of measurement.

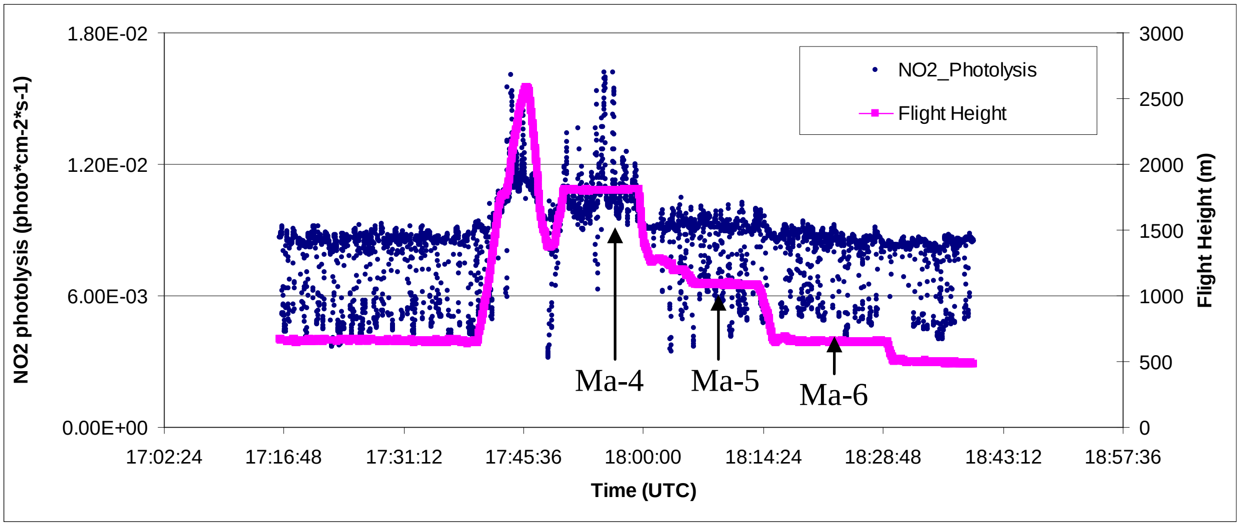


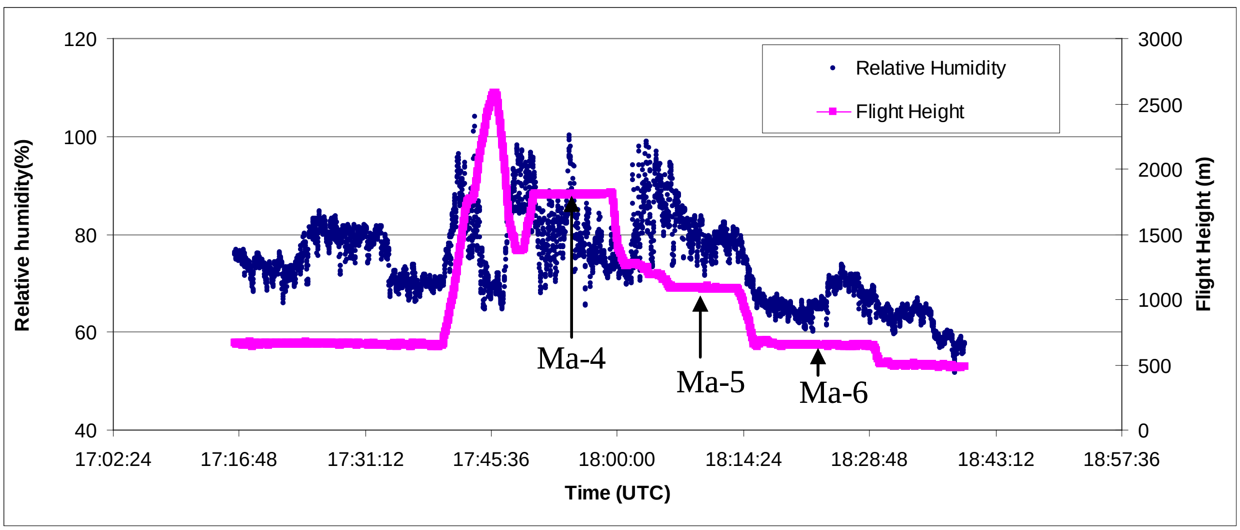


Fig. S8 (a) the observed photolysis rate (left axis, blue dot) and the flight height (right axis, black line). (b) the observed relative humidity (right axis, black cross) and the flight height (left axis, blue line). The corresponding plume transects (Table 3 and Fig. 2) are marked.

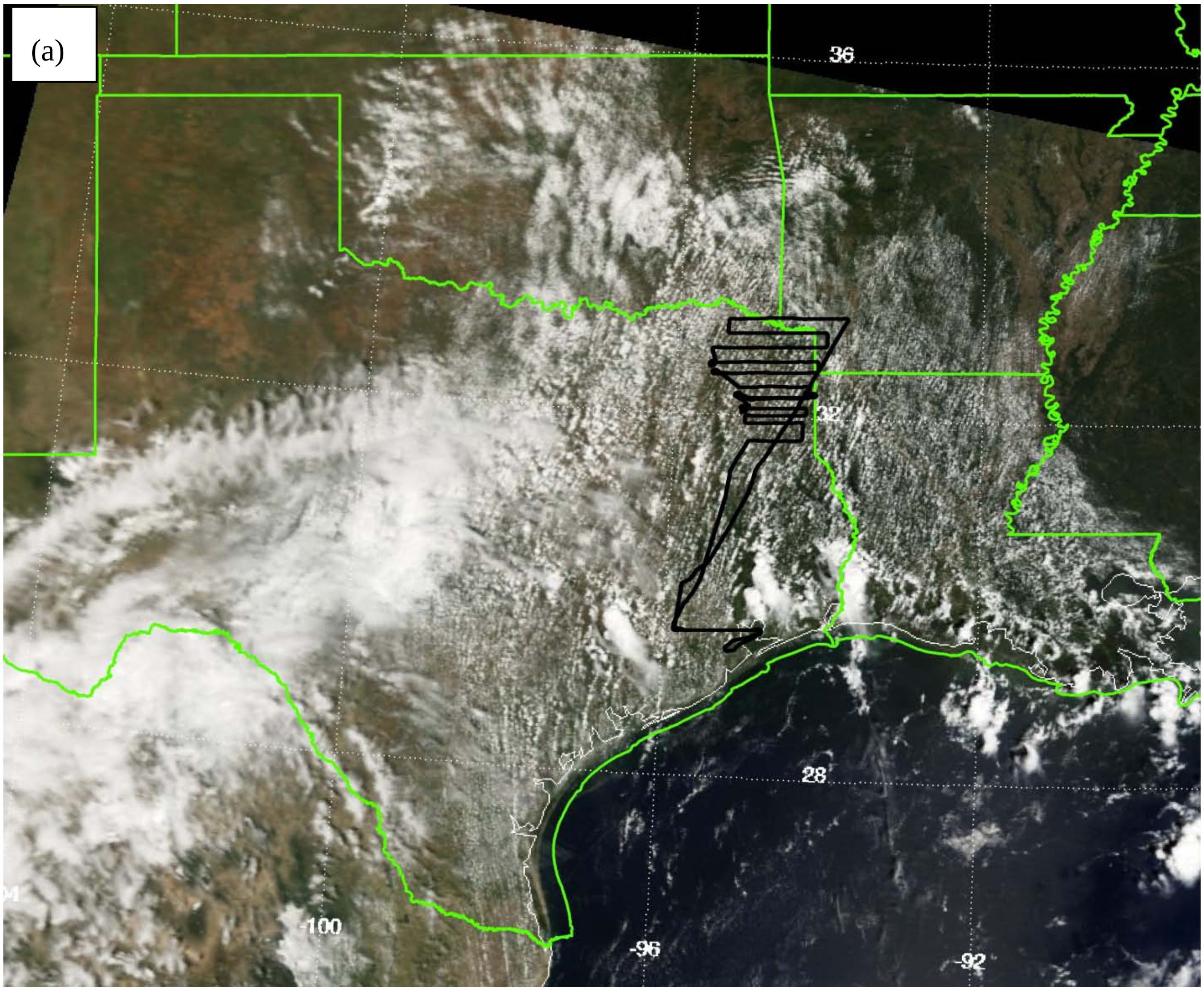

(a)
36
32
28
-100
-96
-92

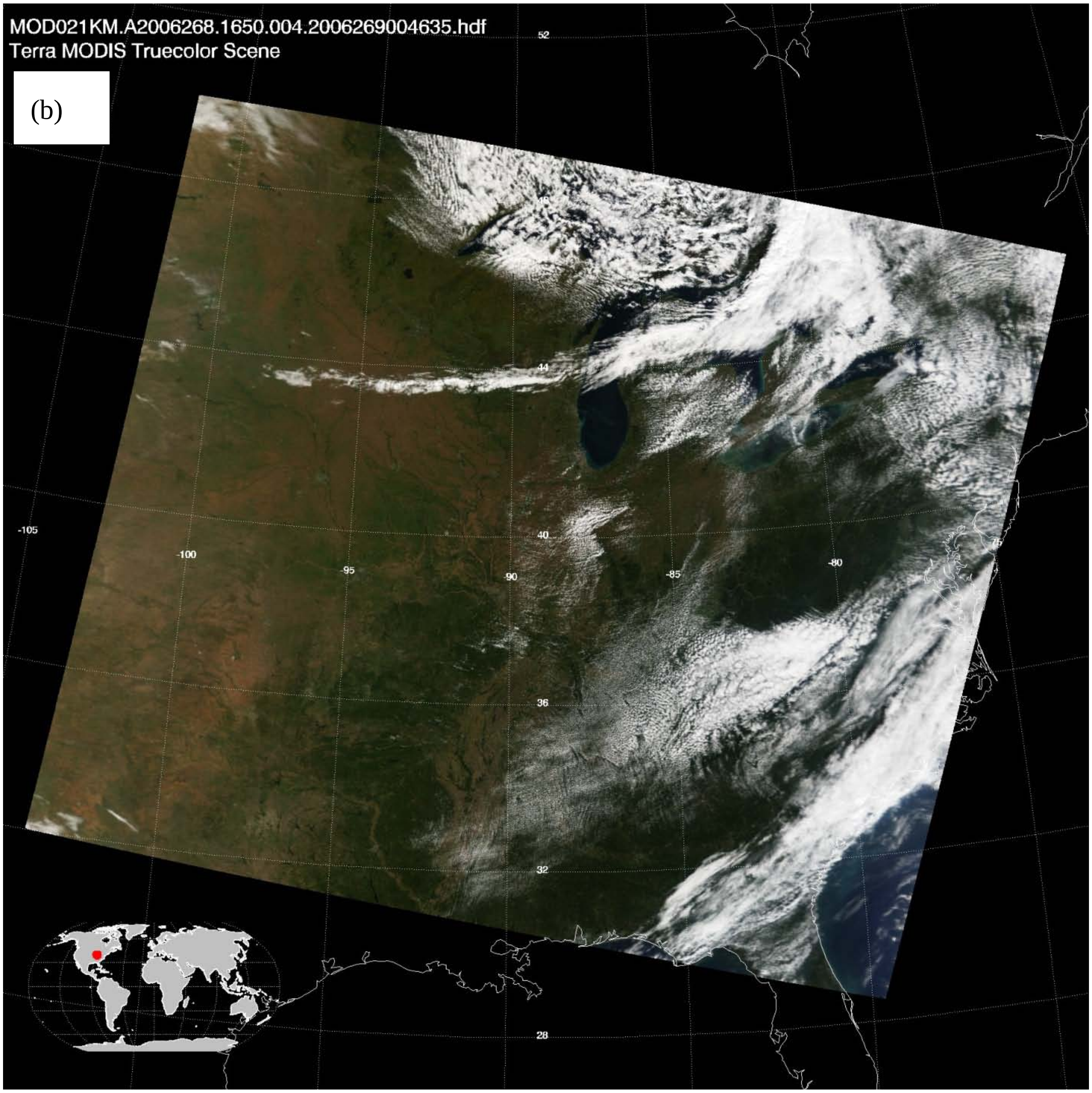
MOD021KM.A2006268.1650.004.2006269004635.hdf
Terra MODIS Truecolor Scene
(b)
52
44
40
36
32
28
-105
-100
-95
-90
-85
-80
-75

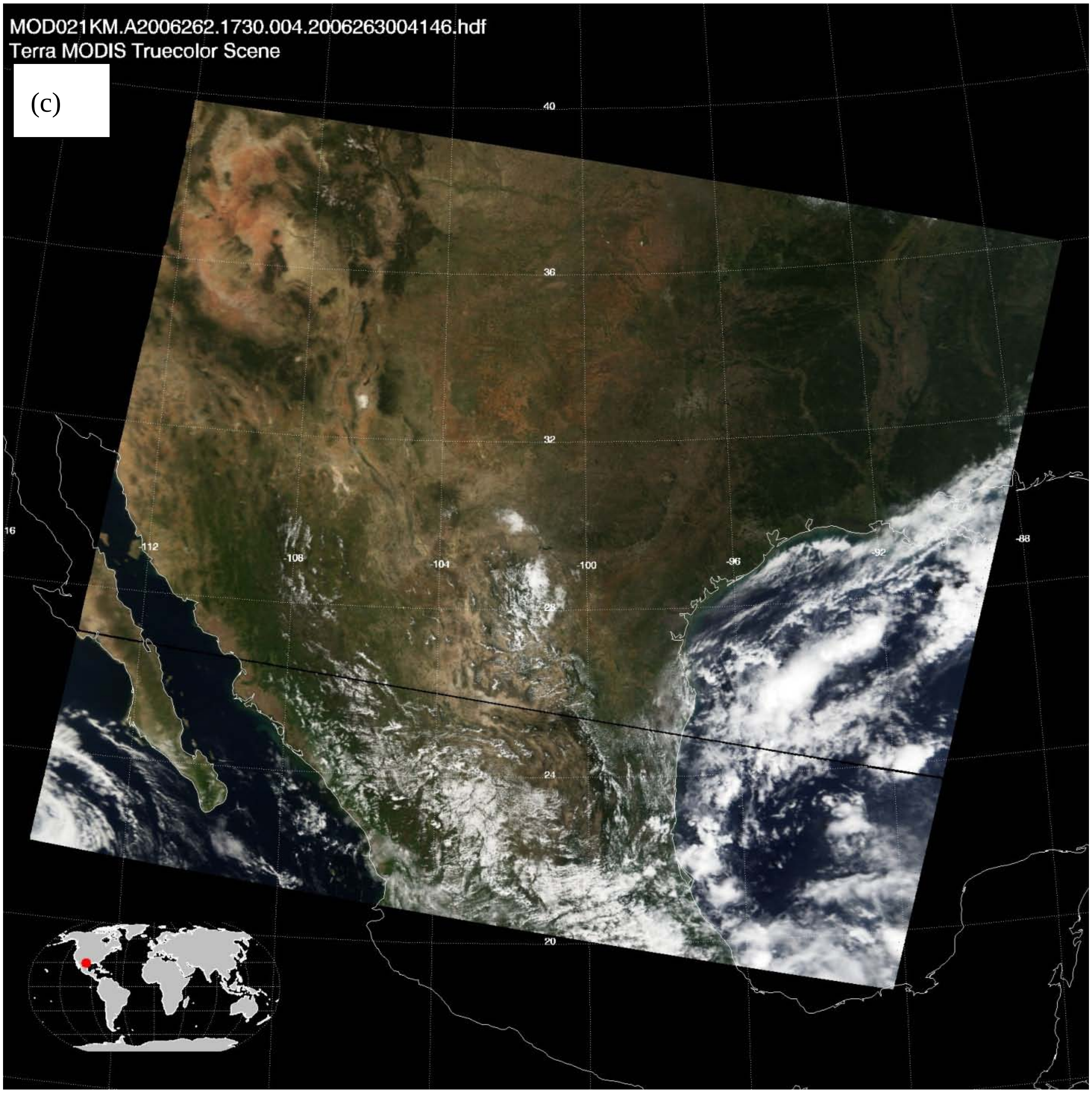


Fig. S9. (a) MODIS true color image (http://modis-atmos.gsfc.nasa.gov/IMAGES/index.html) at 17:00 UTC (local time: 11:00). The black lines indicate the trajectory of the WP-3 path. The WP-3 flew in the early afternoon hours through northeastern Texas covered by sparse clouds. (b) MODIS true color image at 16:50 UTC (local time: 10:50) on September 25; over most areas of Texas, it was clear sky and cloud-free. (c) MODIS true color image at 17:30 UTC (local time: 11:50) on September 19; over most areas of Texas, it was clear sky and cloud-free.

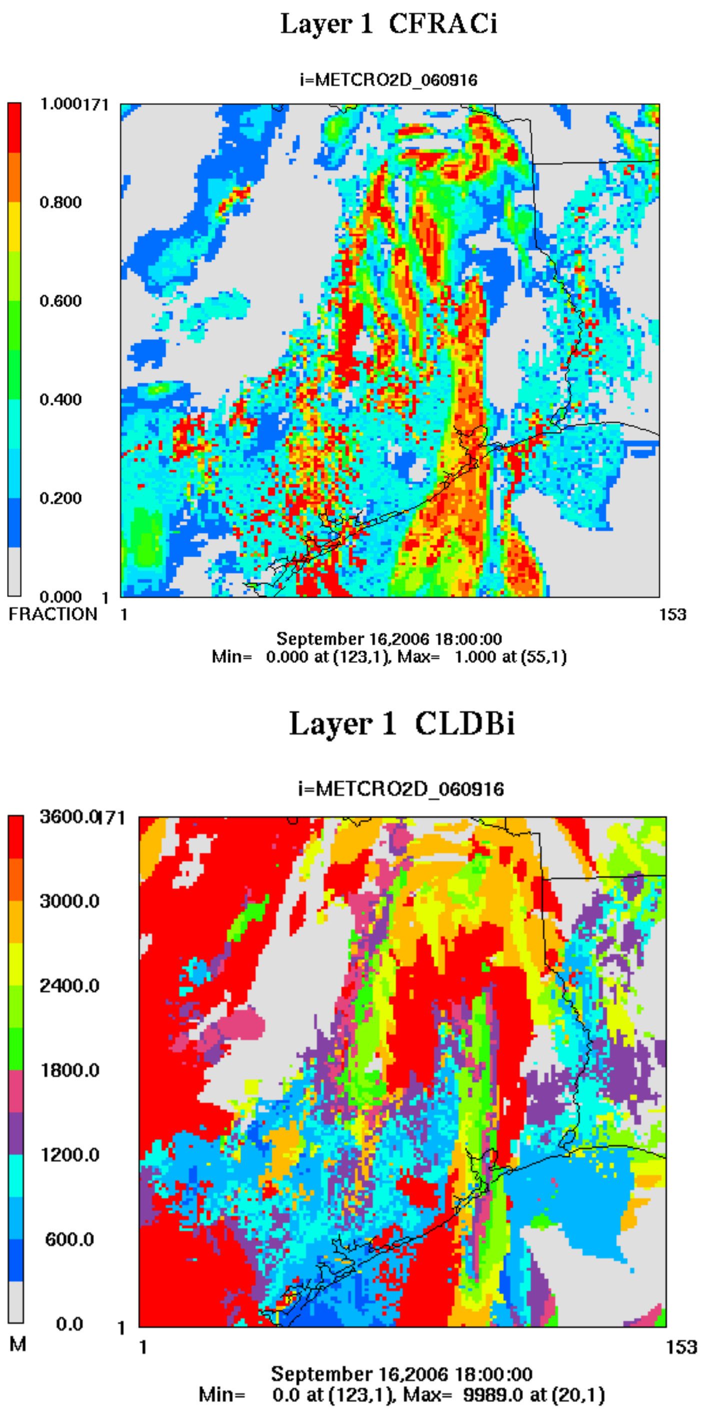


Fig. S10. Modeled (a) cloud cover fraction and (b) cloud bottom height over Texas on September 16, 2006 (18:00 UTC, local time 12:00).

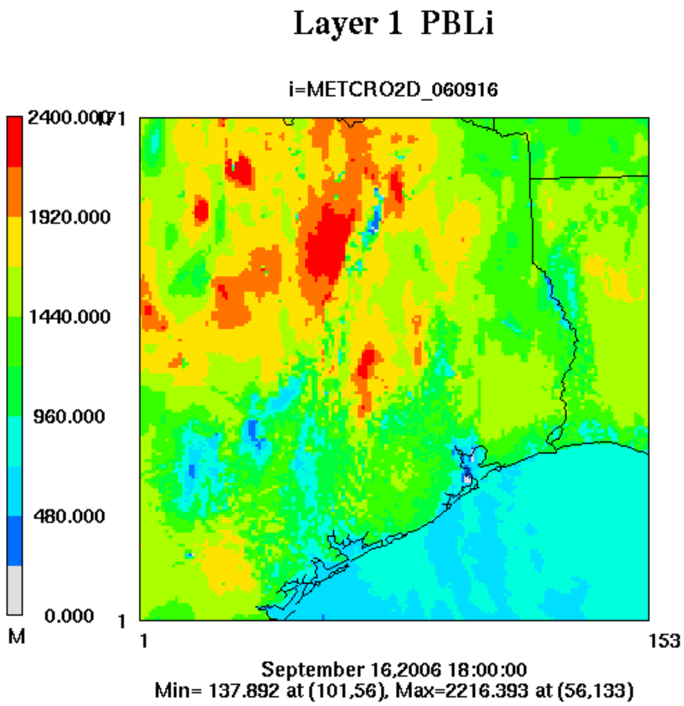


Fig. S11. Modeled planetary boundary layer height at 18:00 UTC (local time: 12:00)

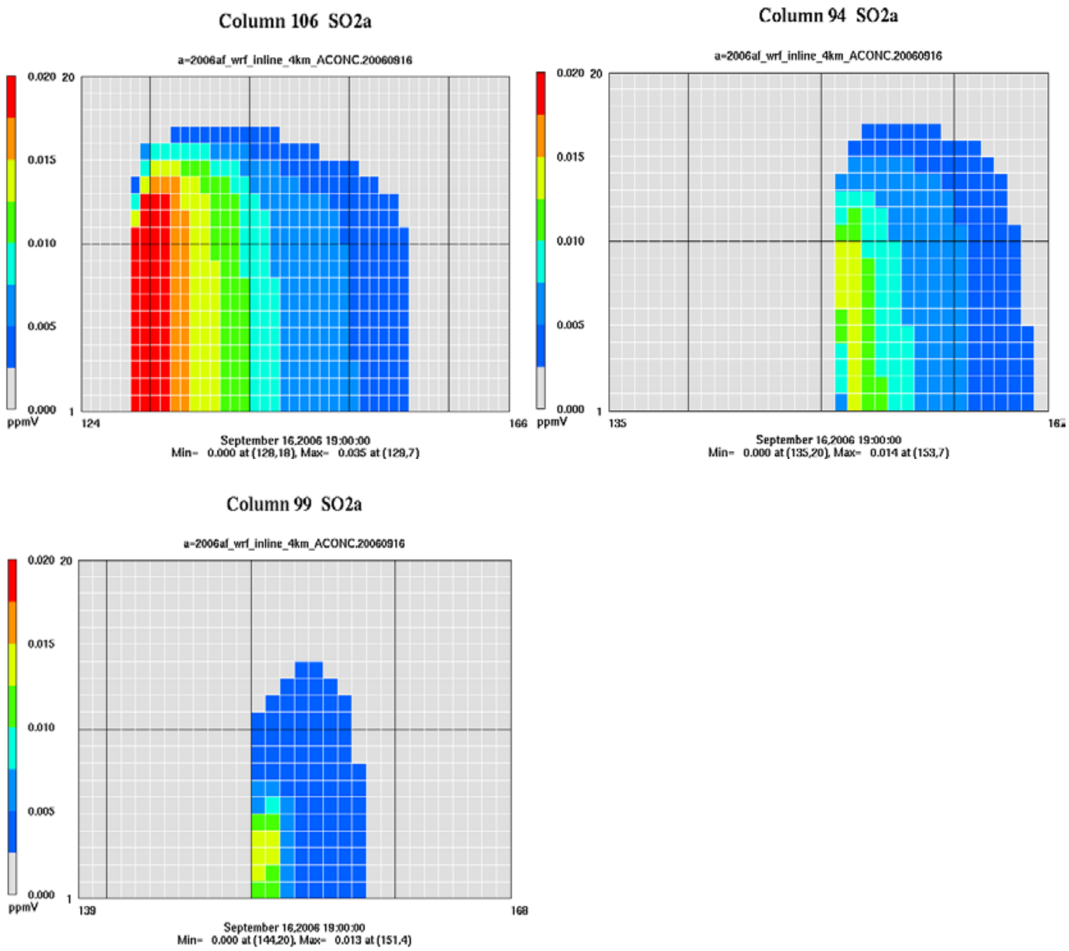


Fig. S12. Vertical distribution ($SO_2$ concentration in ppm unit) of Martin Lake (a), Monticello (b), and Welsh plumes (c) on September 16. Vertical axis is the model layers.

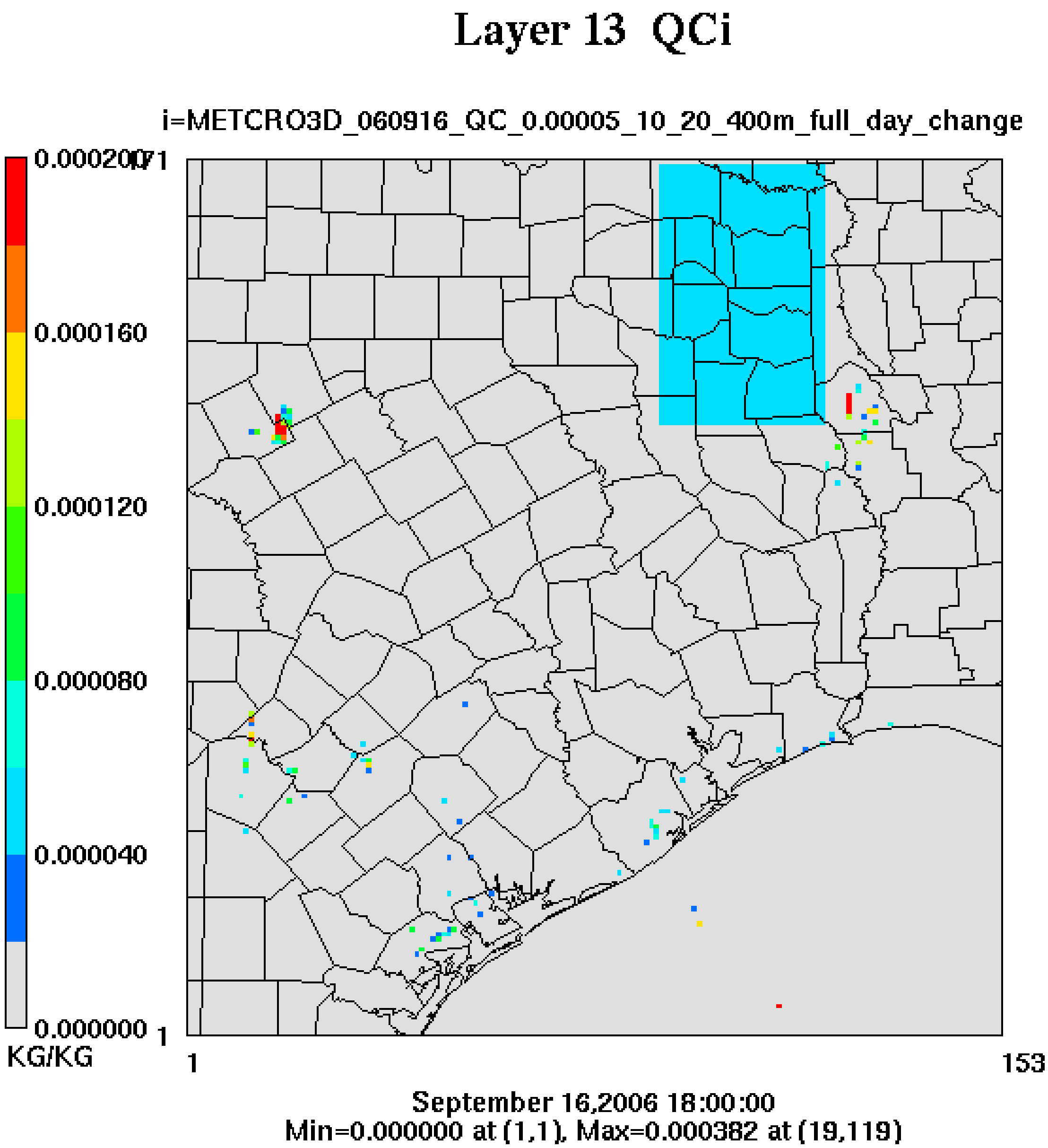


Fig. S13. The region (light blue) for adjusting the cloud liquid water mixing ratio (QC, KG/KG) in the modeling domain. In the northeastern Texas, QC is uniformly set to 0.00005 KG/KG, 0.0005 KG/KG, and 0.005 KG/KG. Layer 13 corresponds to about 1000 m.

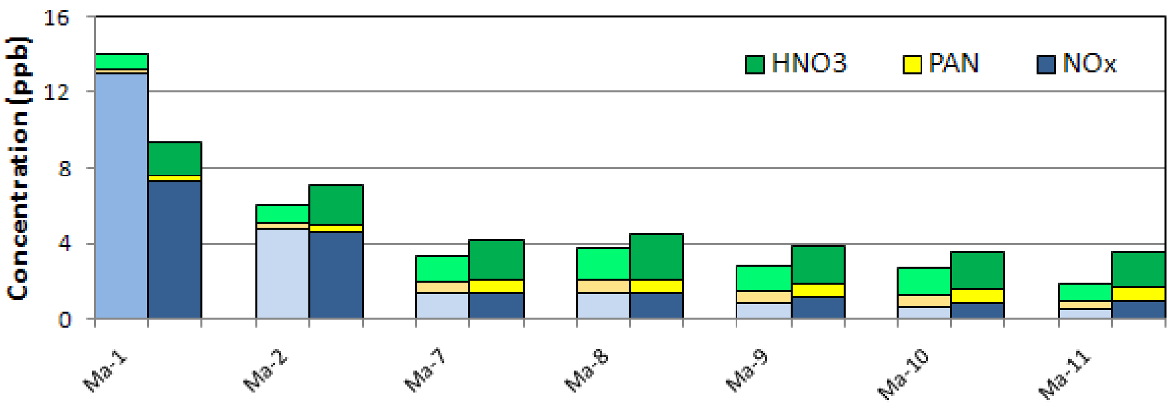


Fig. S14. Concentrations of $HNO_3$ (green), $NO_x$ (blue), and PAN (yellow) at Martin Lake plume transects from observation (left bars with light colors) and model (right bars with dark colors); one of $NO_x$, $HNO_3$, or PAN was not measured at Ma-3, Ma-6, and Ma-12. The observed and modeled concentrations are the average at transects.

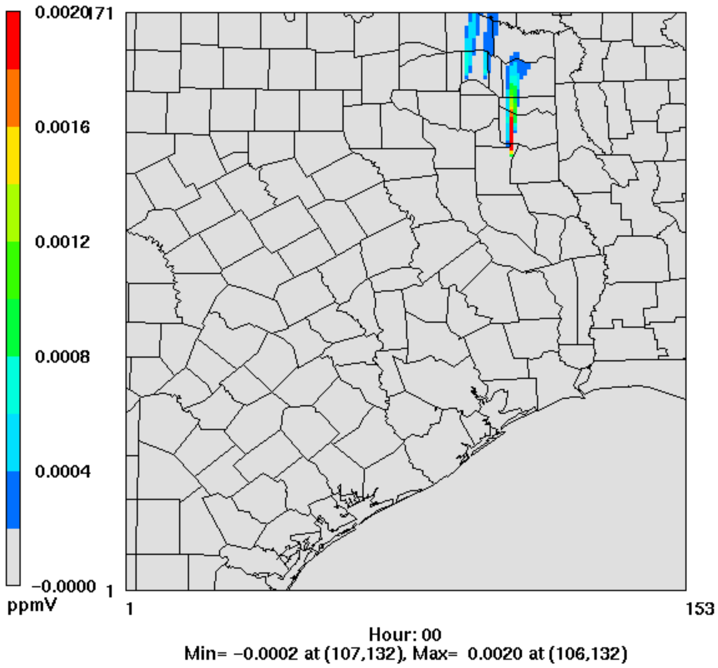


Fig. S15. Difference of ZOC($SO_2$) for Martin Lake, Monticello, and Welsh plumes at layer 10 between the base case and QC_0.05 averaged over 17:00 to 20:00 UTC.

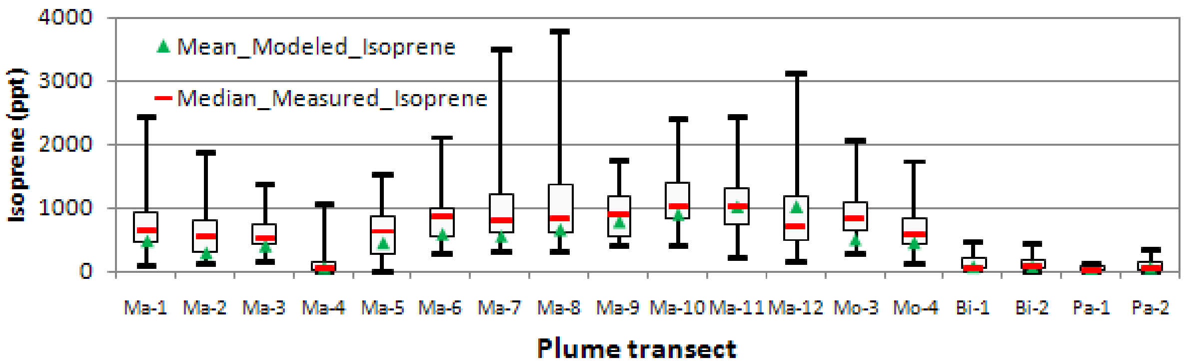


Fig. S16. Modeled (green triangle) and observed (box-and-whiskers) concentration at all transects on 16 and 25 September. The boxes show 25th and 75th percentiles of observations; red lines show medians, and whiskers show minimum and maximum values.

Table S1 Model layer height

| Layer | Height(m) |
|---|---|
| 1 | 43 |
| 2 | 86 |
| 3 | 129 |
| 4 | 172 |
| 5 | 260 |
| 6 | 349 |
| 7 | 436 |
| 8 | 525 |
| 9 | 616 |
| 10 | 706 |
| 11 | 798 |
| 12 | 888 |
| 13 | 1074 |
| 14 | 1266 |
| 15 | 1455 |
| 16 | 1650 |
| 17 | 1851 |
| 18 | 2157 |
| 19 | 2477 |
| 20 | 2904 |
| 21 | 3477 |
| 22 | 4081 |
| 23 | 4994 |
| 24 | 5064 |
| 25 | 6384 |
| 26 | 7165 |
| 27 | 8017 |
| 28 | 8950 |
| 29 | 9981 |
| 30 | 11030 |
| 31 | 12580 |
| 32 | 13441 |
| 33 | 15439 |
| 34 | 18328 |

Table S2. Instruments and time resolution of major gas-phase species discussed

| Species | Reference | Instrument | Time resolution of measurement (second) |
|---|---|---|---|
| $O_3$ | Ryerson et al., 1998 | NO-induced Chemiluminescence (CL) | 1 |
| NO | Ryerson et al., 1999 | $O_3$-induced CL | 1 |
| $NO_2$ | Ryerson et al., 2000 | UV photolysis CL | 1 |
| $HNO_3$ | Neuman et al., 2000 | $SiF_5^-$ Chemical Ionization Mass Spectrometry (CIMS) | 1 |
| $NO_y$ | Ryerson et al., 1999 | Au converter CL | 1 |
| $SO_2$ | Ryerson et al., 1998 | Pulsed UV fluorescence | 1 |
| CO | Holloway et al., 2000 | VUV resonance fluorescence | 1 |
| $CO_2$ | Peischl et al., 2010 | NDIR absorption | 1 |
| Isoprene | de Gouw et al., 2003 | Proton Transfer Reaction Mass Spectrometry (PTRMS) | 17 |
| PAN | Slusher et al., 2004 | CIMS | 2 |

Table S3. Plume transects measured on 16, 19 and 25 September

| Facility | Transect [a] | Distance from plant (km) | Flight height (m) | Average wind speed (m/s) | Plume age [b] (hours) |
|---|---|---|---|---|---|
| Martin Lake | Ma-1 | 17.3 | 660 | 7.4 | 0.7 |
| Martin Lake | Ma-2 | 27.0 | 660 | 6.1 | 1.1 |
| Martin Lake | Ma-3 | 37.1 | 660 | 7.1 | 1.5 |
| Martin Lake | Ma-4 | 52.6 | 1800 | 8.8 | 2.0 |
| Martin Lake | Ma-5 | 52.6 | 1080 | 7.9 | 2.0 |
| Martin Lake | Ma-6 | 52.6 | 640 | 5.4 | 2.0 |
| Martin Lake | Ma-7 | 52.6 | 490 | 6.8 | 2.0 |
| Martin Lake | Ma-8 | 52.6 | 300 | 5.5 | 2.0 |
| Martin Lake | Ma-9 | 67.5 | 660 | 2.9 | 3.4 |
| Martin Lake | Ma-10 | 88.1 | 640 | 4.0 | 4.8 |
| Martin Lake | Ma-11 | 105.7 | 650 | 4.7 | 5.9 |
| Martin Lake | Ma-12 | 115.9 | 650 | 4.2 | 6.6 |
| Monticello | Mo-1 | 7.8 | 640 | 8.0 | 0.3 |
| Monticello | Mo-2 | 27.7 | 650 | 6.3 | 1.2 |
| Monticello | Mo-3 | 47.9 | 650 | 8.1 | 1.6 |
| Monticello | Mo-4 | 67.7 | 660 | 7.8 | 2.4 |
| Welsh | We-1 | 11.5 | 640 | 8.4 | 0.4 |
| Welsh | We-2 | 31.6 | 650 | 5.7 | 1.4 |
| Welsh | We-3 | 51.7 | 650 | 8.9 | 2.0 |
| Welsh | We-4 | 71.8 | 660 | 8.0 | 2.5 |
| Big Brown | Bi-1 | 20.3 | 630 | 4.2 | 1.3 |
| Big Brown/Limestone | Bi-2 | 95.7 | 624 | 6.4 | 3.3 |
| Parish | Pa-1 | 13.5 | 476 | 5.9 | 0.6 |
| Parish | Pa-2 | 43.3 | 482 | 7.0 | 1.2 |
| Parish | Pa-19-1 | 3.2 | 471 | 4.1 | 1.5 |
| Parish | Pa-19-2 | 10.0 | 491 | 5.4 | 4.9 |
| Parish | Pa-19-3 | 12.3 | 462 | 5.0 | 6.1 |
| Parish | Pa-19-4 | 14.5 | 476 | 5.9 | 6.9 |

| | | | | | |
|---|---|---|---|---|---|
| Parish | Pa-19-5 | 20.6 | 488 | 6.2 | 10.6 |

[a] the downwind locations of the plume transects listed in this table are marked in Fig. 2 and Fig. S5 and S6 in supplement

[b] plume age is computed as the distance of plume transect from plant divided by the measured average wind speed at plume transect

Table S4. Background and plume $O_3$ (ppb) and OPE (unitless) from model and observations.

| transect | OBS_$O_3$_BG[a] | MOD_$O_3$_BG[b] | OBS_$\Delta O_3$[c] | MOD_ $\Delta O_3$[d] | OBS_OPE[e] | MOD_OPE[f] |
|---|---|---|---|---|---|---|
| Ma-1 | 30.0 | 46.5 | -2.6 | -0.6 | - | -0.5 |
| Ma-2 | 34.0 | 49.6 | -1.0 | 1.5 | - | 1.9 |
| Ma-3 | 37.3 | 47.0 | 2.4 | 2.0 | 2.6(0.30) | 2.5 |
| Ma-6 | 34.0 | 51.5 | 8.9 | 8.0 | 7.2(0.90) | 4.7 |
| Ma-7 | 34.9 | 52.1 | - | 8.4 | 6.2(0.69) | 4.0 |
| Ma-8 | 35.5 | 52.9 | - | 8.3 | 6.8(0.94) | 4.3 |
| Ma-9 | 37.4 | 51.3 | 9.7 | 9.5 | 6.7(0.80) | 5.5 |
| Ma-10 | 38.3 | 50.3 | 8.9 | 7.0 | 8.7(0.96) | 4.9 |
| Ma-11 | 37.0 | 44.2 | 7.9 | 5.2 | 10.1(0.93) | 4.9 |
| Ma-12 | 37.0 | 45.4 | 7.4 | 5.3 | - | 5.1 |
| Mo-1 | 32.7 | 44.3 | -1.8 | -0.6 | - | -1.0 |
| Mo-2 | 35.1 | 47.6 | 2.0 | 1.3 | 1.4(0.30) | 4.1 |
| Mo-3 | 37.0 | 49.3 | 4.8 | 4.0 | 8.3(0.90) | 5.5 |
| Mo-4 | 36.2 | 48.1 | 4.5 | 2.4 | 10.4(0.94) | 4.9 |
| We-1 | 32.7 | 44.3 | -1.2 | -1.1 | - | -1.9 |
| We-2 | 35.1 | 47.6 | 4.8 | 2.8 | 4.6(0.79) | 4.1 |
| We-3 | 37.0 | 49.3 | 5.3 | 4.0 | 9.4(0.71) | 4.4 |
| We-4 | 36.2 | 48.1 | 7.4 | 5.2 | 10.7(0.75) | 4.6 |
| Bi-1 | - | 44.2 | - | 3.1 | 1.7 (0.75) | 1.5 |
| Bi-2 | - | 46.3 | - | 2.0 | - | 2.9 |
| Pa-1 | - | 52.4 | - | -1.3 | 4.4(0.41) | -6.5 |
| Pa-2 | - | 53.5 | - | 0.4 | 4.0(0.83) | 1.0 |

[a] OBS_$O_3$_BG: observed background $O_3$ (in parentheses, dashes mean no valid value can be found for OBS_$O_3$_BG)

[b] MOD_$O_3$_BG: modeled background $O_3$

[c] OBS_ $\Delta O_3$: OBS_$O_3$_Plume - OBS_$O_3$_BG (in parentheses, dashes mean no valid value can be found for OBS_$\Delta O_3$_BG)

[d] MOD_ $\Delta O_3$: $ZOC_{O3}$ (=$O_{3\ \text{model, base}} - O_{3\ \text{model, zero-out that plant}}$)

[e] OBS_OPE: ozone production efficiency of observed plume from the least square fits of $O_3$ to ($NO_y$-$NO_x$); values in parentheses are the $R^2$ of least square fit of $O_3$ to ($NO_y$-$NO_x$) (in parentheses, dashes mean no valid value can be found for OBS_OPE)

[f] MOD_OPE: ozone production efficiency of modeled plume (=$ZOC_{O3}$/$ZOC_{NOz}$)